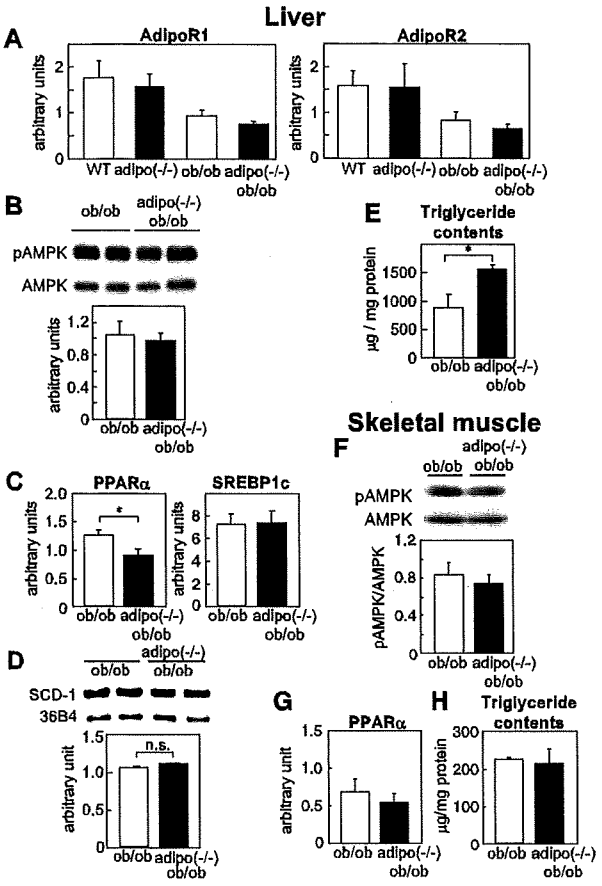


**Fig. 4.** The reduced expressions of the lipogenic genes in the adipo(–/–) mice were no longer seen in the adipo(–/–) mice with a leptin-deficient background.
(A) AdipoR1 and AdipoR2 mRNA expression levels in the liver (n = 3–6). (B) AMPK phosphorylation in the liver (n = 5). (C-D) mRNA levels of PPARalpha, SREBP-1c (C) and SCD-1 (D) in the liver (n = 4–5). (E) Hepatic triglyceride content (n = 5). (F) AMPK phosphorylation in the skeletal muscle (n = 5). (G) PPARalpha expression level in the skeletal muscle (n = 5). (H) Triglyceride content in the skeletal muscle (n = 5). All values are expressed as means ± SEM of data obtained from the analysis of ob/ob (*open bars*) and adipo(–/–)ob/ob mice (*closed bars*). *$p<0.05$.

was observed in the adipo(–/–) mice as compared with that in the wild-type mice (Fig. 3C), suggesting that fatty acid oxidation may be reduced in the liver of the adipo(–/–) mice. The expressions of lipogenic genes such as SREBP-1 (Fig. 3C) and SCD-1 (Fig. 3D) were also significantly down-regulated in the adipo(–/–) mice, and the hepatic triglyceride content was not elevated in the adipo(–/–) mice (Fig. 3E). This unexpected down-regulation of lipogenic genes, which may be explained by the increased leptin sensitivity seen in the adipo(–/–) mice [17], might have prevented the elevation of the triglyceride content in the liver of the adipo(–/–) mice. In the skeletal muscle, we previously reported that the phosphorylation of AMPK was increased in adipo(–/–) mice, presumably due to increased leptin sensitivity [17]. Consistent with this, although the expression of PPARalpha was similar in the wild-type and adipo(–/–) mice (Fig. 3F), the muscle triglyceride content was significantly decreased in the adipo(–/–) mice (Fig. 3G).

### *The reduced expressions of the lipogenic genes observed in the adipo(–/–) mice no longer seen in the adipo(–/–) mice with a leptin-deficient background*

To evaluate the existence of the aforementioned compensatory mechanism in the adipo(–/–) mice, we generated adipo(–/–)ob/ob mice. The expression levels of AdipoR1 and AdipoR2 were similar in the liver of the ob/ob and adipo(–/–)ob/ob mice. Comparison of the wild-type with ob/ob mice, and of the adipo(–/–) with adipo(–/–)ob/ob mice demonstrated a tendency towards reduced expression levels of the adiponectin receptors in the leptin-deficient background (Fig. 4A). Significant decrease of PPARalpha expression was observed in the liver of the adipo(–/–)ob/ob mice (Fig. 4C), as in the liver of the adipo(–/–) mice (Fig. 3C). The expression levels of SREBP-1c (Fig. 4C) and SCD-1 (Fig. 4D) were not altered in the liver of the adipo(–/–)ob/ob mice, unlike in the liver of the adipo(–/–) mice, indicating that the compensatory mechanism in the adipo(–/–) mice was no longer operative in the adipo(–/–)ob/ob mice. In fact, the hepatic triglyceride content was significantly increased in the adipo(–/–)ob/ob mice (Fig. 4E). These data suggest that the leptin pathway might have contributed to the reduced expressions of the lipogenic genes and absence of elevation of the hepatic triglyceride content in the adipo(–/–) mice. In the skeletal muscle, increased phosphorylation of AMPK in the adipo(–/–) was no longer observed in the adipo(–/–)ob/ob mice (Fig. 4F). The expression level of PPARalpha (Fig. 4G) and the triglyceride content (Fig. 4H) were also unaltered in the skeletal muscle of adipo(–/–)ob/ob mice.

## Discussion

In the present study, we investigated the molecular mechanisms of the insulin resistance in adipo(–/–) mice. Adipo(–/–) mice showed hepatic, but not muscle, insulin resistance. Insulin-stimulated tyrosine phosphorylation of IRS-1 and IRS-2 was impaired in the liver of the adipo(–/–) mice, despite the absence of any change in the hepatic triglyceride content. One of the underlying mechanisms responsible for this may be the increased phosphorylation of the serine/threonine residue of IRS-1 in the liver of these mice, which is currently under investigation. Moreover, the IRS-2 protein level was also significantly decreased in the adipo(–/–) mice; as a result, insulin-stimulated phosphorylation of Akt was significantly decreased in these mice. In the skeletal muscle, on the other hand, insulin-stimulated phosphorylation of IRS-1 and Akt was similar in degree between the wild-type and adipo(–/–) mice. In fact, while the EGP and expression levels of PEPCK and G6Pase were increased, the Rd was not found to be significantly changed in the adipo(–/–) mice during the euglycemic-hyperinsulinemic clamp study.

Triglyceride content in the liver was not increased in the adipo(–/–) mice, despite the decrease in PPARalpha expression involved in lipid combustion, since the expressions of lipogenic genes such as SREBP-1 and SCD-1 were decreased in association with the increased leptin sensitivity. Consistent with this, down-regulation of SREBP-1 and SCD-1 observed in the adipo(–/–) mice was no longer observed in the adipo(–/–)ob/ob mice, and the hepatic triglyceride content was significantly increased in the adipo(–/–)ob/ob mice as compared with that in the ob/ob mice. On the other hand, the triglyceride content in the skeletal muscle was significantly decreased in the adipo(–/–) mice, probably due to the up-regulated muscle AMPK activity associated with the increased leptin sensitivity in these mice [17]. In fact, the increase in AMPK activity [17] and decrease triglyceride content in the skeletal muscle were no longer observed in the adipo(–/–)ob/ob mice. Therefore, increase in the leptin actions appears to compensate for the adiponectin deficiency in both the liver and the skeletal muscle of the adipo(–/–) mice, accounting for the unexpected absence of a increase in the hepatic triglyceride content and rather decreased muscle triglyceride content in the adipo(–/–) mice [13].

Why was the degree of insulin resistance different between the liver and skeletal muscle of the adipo(–/–) mice? We recently demonstrated that adiponectin induces the expression of IRS-2 in the liver (Awazawa M, Ueki K and Kadowaki T, manuscript in preparation). IRS-2 is a major IRS in the liver, but not in the skeletal muscle [25], suggesting that the reduction of IRS-2 due to adiponectin deficiency may have little effect on the insulin signaling in the skeletal muscle of adipo(–/–) mice.

A similar degree of phosphorylation of AMPK was seen in the liver of the wild-type and adipo(–/–) mice, even though adiponectin is known to activate AMPK [9, 10]. SCD-1 expression was down-regulated in the adipo(–/–) mice. Increased phosphorylation of AMPK has been reported in the liver of SCD-1-knockout mice [26]. It is suggested that the down-regulation of AMPK resulting from adiponectin deficiency may be balanced by the up-regulation of AMPK occurring as a result of the decreased SCD-1 expression, resulting in the absence of any net change in the phosphorylation level of AMPK in the liver of the adipo(–/–) mice. In Nawrocki's study, there appeared to be no differences in the phosphorylation level and activity of AMPK between the wild-type and adipo(–/–) mice [16].

In conclusion, adipo(–/–) mice showed impaired insulin signaling in the liver to cause hepatic insulin resistance, however, no increase in the triglyceride content was observed in either the liver or the skeletal muscle, presumably on account of the increased leptin sensitivity.

## Acknowledgements

We thank Dr. R. Suzuki for his helpful suggestions. We are grateful to Eri Yoshida-Nagata, Ayumi Nagano, Miharu Nakashima, Namiko Kasuga, Yuko Miki, Hiroshi Chiyonobu, Miyoko Suzuki and Masahiro Nakamaru for their excellent technical assistance and animal care. This work was supported by a grant from the Program for Promotion of Fundamental Studies in Health Sciences of the Organization for Pharmaceutical Safety and Research of Japan (to T.K.), and a grant from the Sankyo Foundation of Life Science (to N.K.).

## References


1. Hug C, Lodish HF (2005) The role of the adipocyte hormone adiponectin in cardiovascular disease. *Curr Opin Pharmacol* 5: 129–134.
2. Scherer PE (2006) Adipose tissue: from lipid storage compartment to endocrine organ. *Diabetes* 55: 1537–1545.
3. Matsuzawa Y (2006) The metabolic syndrome and adipocytokines. *FEBS Lett* 580: 2917–2921.
4. Kadowaki T, Yamauchi T, Kubota N, Hara K, Ueki K, Tobe K (2006) Adiponectin and adiponectin receptors in insulin resistance, diabetes, and the metabolic syndrome. *J Clin Invest* 116: 1784–1792.
5. Fruebis J, Tsao TS, Javorschi S, Ebbets-Reed D, Erickson MR, Yen FT, Bihain BE, Lodish HF (2001) Proteolytic cleavage product of 30-kDa adipocyte complement-related protein increases fatty acid oxidation in muscle and causes weight loss in mice. *Proc Natl Acad Sci USA* 98: 2005–2010.
6. Yamauchi T, Kamon J, Waki H, Terauchi Y, Kubota N, Hara K, Mori Y, Ide T, Murakami K, Tsuboyama-Kasaoka N, Ezaki O, Akanuma Y, Gavrilova O, Vinson C, Reitman ML, Kagechika H, Shudo K, Yoda M, Nakano Y, Tobe K, Nagai R, Kimura S, Tomita M, Froguel P, Kadowaki T (2001) The fat-derived hormone adiponectin reverses insulin resistance associated with both lipoatrophy and obesity. *Nat Med* 7: 941–946.
7. Berg AH, Combs TP, Du X, Brownlee M, Scherer PE (2001) The adipocyte-secreted protein Acrp30 enhances hepatic insulin action. *Nat Med* 7: 947–953.
8. Combs TP, Berg AH, Obici S, Scherer PE, Rossetti L (2001) Endogenous glucose production is inhibited by the adipose-derived protein Acrp30. *J Clin Invest* 108: 1875–1881.
9. Yamauchi T, Kamon J, Minokoshi Y, Ito Y, Waki H, Uchida S, Yamashita S, Noda M, Kita S, Ueki K, Eto K, Akanuma Y, Froguel P, Foufelle F, Ferre P, Carling D, Kimura S, Nagai R, Kahn BB, Kadowaki T (2002) Adiponectin stimulates glucose utilization and fatty-acid oxidation by activating AMP-activated protein kinase. *Nat Med* 8: 1288–1295.
10. Tomas E, Tsao TS, Saha AK, Murrey HE, Zhang CC, Itani SI, Lodish HF, Ruderman NB (2002) Enhanced muscle fat oxidation and glucose transport by ACRP30 globular domain: Acetyl-CoA carboxylase inhibition and AMP-activated protein kinase activation. *Proc Natl Acad Sci USA* 99: 16309–16313.
11. Kersten S, Desvergne B, Wahli W (2000) Roles of PPARs in health and disease. *Nature* 405: 421–424.
12. Yamauchi T, Kamon J, Waki H, Imai Y, Shimozawa N, Hioki K, Uchida S, Ito Y, Takakuwa K, Matsui J, Takata M, Eto K, Terauchi Y, Komeda K, Tsunoda M, Murakami K, Ohnishi Y, Naitoh T, Yamamura K, Ueyama Y, Froguel P, Kimura S, Nagai R, Kadowaki T (2003) Globular adiponectin protected ob/ob mice from diabetes and apoE-deficient mice from atherosclerosis. *J Biol Chem* 278: 2461–2468.
13. Kubota N, Terauchi Y, Yamauchi T, Kubota T, Moroi M, Matsui J, Eto K, Yamashita T, Kamon J, Satoh H, Yano W, Froguel P, Nagai R, Kimura S, Kadowaki T, Noda T (2002) Disruption of adiponectin causes insulin resistance and neointimal formation. *J Biol Chem* 277: 25863–25866.
14. Maeda N, Shimomura I, Kishida K, Nishizawa H, Matsuda M, Nagaretani H, Furuyama N, Kondo H, Takahashi M, Arita Y, Komuro R, Ouchi N, Kihara S, Tochino Y, Okutomi K, Horie M, Takeda S, Aoyama T, Funahashi T, Matsuzawa Y (2002) Diet-induced insulin resistance in mice lacking adiponectin/ACRP30. *Nat Med* 8: 731–737.
15. Ma K, Cabrero A, Saha PK, Kojima H, Li L, Chang BH, Paul A, Chan L (2002) Increased beta-Oxidation but no insulin resistance or glucose intolerance in mice lacking adiponectin. *J Biol Chem* 277: 34658–34661.
16. Nawrocki AR, Rajala MW, Tomas E, Pajvani UB, Saha AK, Trumbauer ME, Pang Z, Chen AS, Ruderman NB, Chen H, Rossetti L, Scherer PE (2006) Mice lacking adiponectin show decreased hepatic insulin sensitivity and reduced responsiveness to peroxisome proliferator-activated receptor γ agonists. *J Biol Chem* 281: 2654–2660.
17. Kubota N, Yano W, Ueki K, Yamauchi T, Okamoto S, Shiuchi T, Kubota T, Okamoto M, Takamoto I, Satoh H, Kita S, Tsuchida A, Moroi M, Sugi K, Kondo T, Araki E, Aburatani H, Suzuki R, Terauchi Y, Tobe K, Ezaki O, Ueta Y, Noda T, Nagai R, Minokoshi Y, Kadowaki T (2007) Adiponectin stimulates AMP-activated protein kinase in the hypothalamus and increases food intake. *Cell Metab* 6: 55–68.
18. Cohen P, Miyazaki M, Socci ND, Hagge-Greenberg A, Liedtke W, Soukas AA, Sharma R, Hudgins LC, Ntambi JM, Friedman JM (2002) Role for stearoyl-CoA desaturase-1 in leptin-mediated weight loss. *Science* 297: 240–243.
19. Tobe K, Suzuki R, Aoyama M, Yamauchi T, Kamon J, Kubota N, Terauchi Y, Matsui J, Akanuma Y, Kimura S, Tanaka J, Abe M, Ohsumi J, Nagai R, Kadowaki T (2001) Increased expression of the sterol regulatory element-binding protein-1 gene in insulin receptor substrate-$2^{-/-}$ mouse liver. *J Biol Chem* 276: 38337–38340.
20. Minokoshi Y, Kim YB, Peroni OD, Fryer LG, Muller C, Carling D, Kahn BB (2002) Leptin stimulates fatty-acid oxidation by activating AMP-activated protein kinase. *Nature* 415: 339–343.
21. Kubota N, Terauchi Y, Kubota T, Kumagai H, Itoh S,

Satoh H, Yano W, Ogata H, Tokuyama K, Takamoto I, Mineyama T, Ishikawa M, Moroi M, Sugi K, Yamauchi T, Ueki K, Tobe K, Noda T, Nagai R, Kadowaki T (2006) Pioglitazone ameliorates insulin resistance and diabetes by both adiponectin-dependent and -independent pathways. *J Biol Chem* 281: 8748–8755.

22. Matsui J, Terauchi Y, Kubota N, Takamoto I, Eto K, Yamashita T, Komeda K, Yamauchi T, Kamon J, Kita S, Noda M, Kadowaki T (2004) Pioglitazone reduces islet triglyceride content and restores impaired glucose-stimulated insulin secretion in heterozygous peroxisome proliferator-sctivated receptor-γ-deficient mice on a high-fat diet. *Diabetes* 53: 2844–2854.
23. Kubota N, Terauchi Y, Tobe K, Yano W, Suzuki R, Ueki K, Takamoto I, Satoh H, Maki T, Kubota T, Moroi M, Okada-Iwabu M, Ezaki O, Nagai R, Ueta Y, Kadowaki T, Noda T (2004) Insulin receptor substrate 2 plays a crucial role in β cells and the hypothalamus. *J Clin Invest* 114: 917–927.
24. Yamauchi T, Kamon J, Ito Y, Tsuchida A, Yokomizo T, Kita S, Sugiyama T, Miyagishi M, Hara K, Tsunoda M, Murakami K, Ohteki T, Uchida S, Takekawa S, Waki H, Tsuno NH, Shibata Y, Terauchi Y, Froguel P, Tobe K, Koyasu S, Taira K, Kitamura T, Shimizu T, Nagai R, Kadowaki T (2003) Cloning of adiponectin receptors that mediate antidiabetic metabolic effects. *Nature* 423: 762–769.
25. Kubota N, Tobe K, Terauchi Y, Eto K, Yamauchi T, Suzuki R, Tsubamoto Y, Komeda K, Nakano R, Miki H, Satoh S, Sekihara H, Sciacchitano S, Lesniak M, Aizawa S, Nagai R, Kimura S, Akanuma Y, Taylor SI, Kadowaki T (2000) Disruption of insulin receptor substrate 2 causes type 2 diabetes because of liver insulin resistance and lack of compensatory β-cell hyperplasia. *Diabetes* 49: 1880–1889.
26. Dobrzyn P, Dobrzyn A, Miyazaki M, Cohen P, Asilmaz E, Hardie DG, Friedman JM, Ntambi JM (2004) Stearoyl-CoA desaturase 1 deficiency increases fatty acid oxidation by activating AMP-activated protein kinase in liver. *Proc Natl Acad Sci USA* 101: 6409–6414.

nature medicine

# SUMOylation of Krüppel-like transcription factor 5 acts as a molecular switch in transcriptional programs of lipid metabolism involving PPAR-δ

Yumiko Oishi[1,2], Ichiro Manabe[1,3], Kazuyuki Tobe[4,5], Mitsuru Ohsugi[4], Tetsuya Kubota[2,4], Katsuhito Fujiu[1], Koji Maemura[1], Naoto Kubota[2,4], Takashi Kadowaki[2,4] & Ryozo Nagai[1]

**Obesity and metabolic syndrome are increasingly recognized as major risk factors for cardiovascular disease. Herein we show that Krüppel-like transcription factor 5 (KLF5) is a crucial regulator of energy metabolism. *Klf5*$^{+/-}$ mice were resistant to high fat–induced obesity, hypercholesterolemia and glucose intolerance, despite consuming more food than wild-type mice. This may in part reflect their enhanced energy expenditure. Expression of the genes involved in lipid oxidation and energy uncoupling, including those encoding carnitine-palmitoyl transferase-1b (*Cpt1b*) and uncoupling proteins 2 and 3 (*Ucp2* and *Ucp3*), was upregulated in the soleus muscles of *Klf5*$^{+/-}$ mice. Under basal conditions, KLF5 modified with small ubiquitin-related modifier (SUMO) proteins was associated with transcriptionally repressive regulatory complexes containing unliganded peroxisome proliferator–activated receptor-δ (PPAR-δ) and co-repressors and thus inhibited *Cpt1b*, *Ucp2* and *Ucp3* expression. Upon agonist stimulation of PPAR-δ, KLF5 was deSUMOylated, and became associated with transcriptional activation complexes containing both the liganded PPAR-δ and CREB binding protein (CBP). This activation complex increased the expression of *Cpt1b*, *Ucp2* and *Ucp3*. Thus, SUMOylation seems to be a molecular switch affecting function of KLF5 and the transcriptional regulatory programs governing lipid metabolism.**



A proper balance between energy intake and energy expenditure is crucial for maintenance of normal body weight. This energy homeostasis is intricately regulated despite variations in access to nutrition and in the demands for physical activity and thermogenesis[1,2]. Skeletal muscle accounts for >30% of energy expenditure and is the primary site of insulin-stimulated glucose uptake, disposal and storage; it also regulates cholesterol efflux and strongly influences metabolism by modulating circulating and stored lipid flux[3]. Skeletal muscle is also heavily innervated by the sympathetic nervous system and seems to be a major target of neural control of energy expenditure[1]. Consequently, dysregulation of energy metabolism in skeletal muscle is a key component of systemic metabolic dysfunction. For instance, a growing body of evidence suggests that defects in fatty acid oxidation probably precede the obese diabetic state[4]. However, the molecular mechanisms underlying the disruption of energy metabolism in skeletal muscle remain poorly understood[5].

Previous studies have extensively documented the intricate transcriptional control mechanisms affecting fatty acid synthesis and storage[6–8]. By contrast, transcriptional regulation of fatty acid oxidation is still only poorly understood, though the transcription factors PPARs, ERRα, Foxa2 and C/EBPs are known to be involved[9–11]. PPAR-δ (also known as PPAR-β) is the predominant PPAR isoform expressed in skeletal muscle, and selective ablation of *Ppard* in skeletal muscle diminishes the oxidative capacity of this tissue, thus leading to the development of obesity and glucose intolerance[12]. Activation of PPAR with the specific agonist GW501516, however, coordinately upregulates expression of genes involved in fatty acid oxidation and energy uncoupling, which markedly diminishes weight gain while increasing $O_2$ consumption in mice fed a high-fat diet[13–15]. Likewise, skeletal muscle–specific overexpression of an activated form of PPAR-δ protects mice from diet-induced obesity[16]. As a result, PPAR-δ is now considered to be an attractive target for treatment of metabolic syndrome.

Even so, it remains unclear how PPAR-δ functions within the transcriptional regulatory programs that govern lipid catabolism. It has been shown in macrophages that unliganded PPAR-δ represses expression of key genes encoding components of the fatty acid oxidation pathway, and deletion of *Ppard* results in derepression of those genes[17]. Moreover, *in vitro* studies have shown that unliganded PPAR-δ represses transcription by interacting with corepressors and histone deacetylases[18,19]. This repressive activity may contribute to the dynamic regulation of transcription that occurs in response to ligands

[1]Department of Cardiovascular Medicine, Graduate School of Medicine, The University of Tokyo, 7-3-1, Hongo, Bunkyo, Tokyo 113-8655, Japan. [2]Clinical Nutrition Program, National Institute of Health and Nutrition, 1-23-1, Toyama, Shinjuku, Tokyo 162-8636, Japan. [3]Nano-Bioengineering Education Program and [4]Department of Metabolic Diseases, Graduate School of Medicine, The University of Tokyo, 7-3-1, Hongo, Bunkyo, Tokyo 113-8655, Japan. [5]First Department of Internal Medicine, University of Toyama, 2630 Sugitani, Toyama 930-0194, Japan. Correspondence should be addressed to I.M. (manabe-tky@umin.ac.jp) or R.N. (nagai-tky@umin.ac.jp).

Received 20 February; accepted 20 March; published online 25 May 2008; doi:10.1038/nm1756

and other signals. However, the mechanisms involved and the molecular components that mediate such dynamic transcriptional control have not been identified, nor has the role of this machinery in the control of lipid metabolism.

SUMO proteins are moieties that are conjugated via an enzymatic cascade to lysine residues in a variety of target proteins[20]. SUMO precursors are processed by SUMO-specific proteases and activated by the E1 enzyme. SUMOs are then transferred to the E2 conjugating enzyme Ubc9, and with the help of an E3 ligase such as PIAS, SUMOs are ligated to a substrate. Because SUMOs can be deconjugated from target proteins by SUMO-specific SENP family proteases, SUMOylation is reversible and highly dynamic, and it is known to suppress transcription in most cases[21]. Several transcription factors involved in energy metabolism have been shown to be modified by SUMOylation, including PPAR-γ (ref. 22), C/EBPs (ref. 23) and SREBPs (ref. 24), although the effect of SUMOylation of those transcription factors on energy metabolism remains unknown.

KLF5 is a member of the large KLF family of transcription factors[25]. KLF5 plays a key part in the pathogenesis of cardiovascular diseases such as atherosclerosis and cardiac hypertrophy and fibrosis by mediating tissue remodeling in response to external stresses[26,27]. KLF5 is also involved in adipocyte differentiation programs through its interaction with C/EBP-β and C/EBP-δ and through transactivation of *Pparg2*, encoding PPAR-$\gamma_2$[28]. Its role in the regulation of metabolism in adult animals has not yet been addressed, however.

Our aim in the present study was to gain insight into the role of KLF5 in regulating the expression of genes involved in lipid metabolism and to better understand how the activity of KLF5 itself is regulated. Our findings show that KLF5 is a unique regulator of lipid metabolism and that its SUMOylation within transcription factor complexes that also contain PPAR-δ serves as a molecular switch to repress or activate genes involved in lipid catabolism in response to PPAR-δ ligand and other signals.

## RESULTS

### *Klf5*$^{+/-}$ mice are protected from diet-induced obesity

As we reported previously, *Klf5*$^{+/-}$ mice showed retarded white adipose tissue (WAT) development during the first postnatal week; however, they developed normally thereafter when fed with chow diet[28], so that by 3 weeks after birth, the body weights of *Klf5*$^{+/-}$mice did not significantly differ from those of their wild-type littermates (**Supplementary Fig. 1a** online). When fed a high-fat diet, in contrast, *Klf5*$^{+/-}$ mice gained significantly less weight than wild-type littermates (**Fig. 1a**). Although the lean body masses and heart weights of

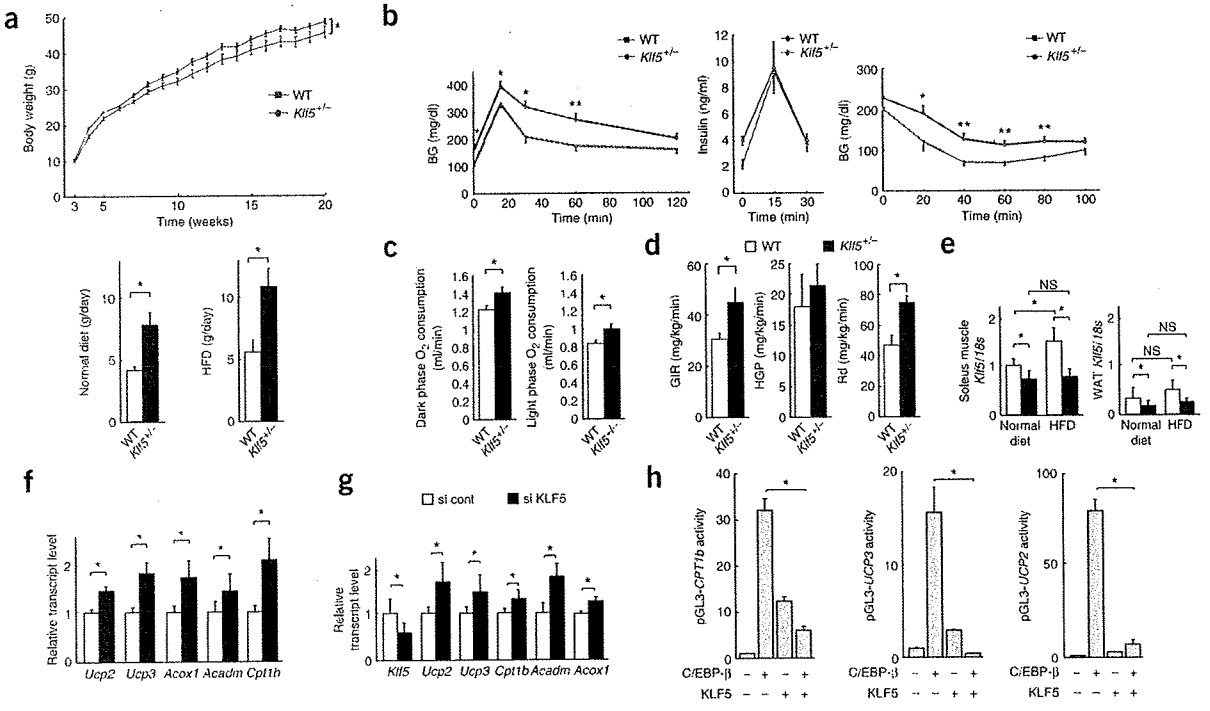


**Figure 1** *Klf5*$^{+/-}$ mice are protected from diet-induced obesity and metabolic dysfunction. (**a**) Top, body weights of wild-type (WT) and *Klf5*$^{+/-}$ mice fed a high-fat diet for 17 weeks ($n = 13$ each, $^*P < 0.05$ two-way ANOVA). Bottom, food intake by 8-week-old mice on a normal chow diet or high-fat diet (HFD) measured every day for 7 d. (**b**) Blood glucose (BG, left) and serum insulin (center) during oral glucose tolerance test and BG during insulin tolerance test (right) in mice fed a HFD for 12 weeks ($n = 13$ each). (**c**) Oxygen consumption under fasting conditions in 18-week-old WT and *Klf5*$^{+/-}$ mice ($n = 10$ each). (**d**) Glucose infusion rates (GIR), hepatic glucose production (HGP) and rates of glucose disappearance (Rd) in a hyperinsulinemic euglycemic clamp study in WT and *Klf5*$^{+/-}$ mice fed a HFD for 8 weeks (WT, $n = 8$; *Klf5*$^{+/-}$, $n = 7$). (**e**) Expression of *Klf5* mRNA in soleus muscle (left) and epididymal WAT (right) in WT and *Klf5*$^{+/-}$ mice fed either normal chow diet or a HFD for 12 weeks ($n = 6$, each genotype). The level of expression was normalized to the level of *18s* rRNA obtained for each condition. The normalized expression levels were then further normalized with respect to the levels in soleus muscle in WT mice fed normal diet. (**f**) Expression of mRNA involved in energy metabolism in soleus muscle in WT and *Klf5*$^{+/-}$ mice fed a HFD. Expression levels were normalized with respect to the levels in WT mice ($n = 6$ each). (**g**) C2C12 myotubes were transfected with either *Klf5*-siRNA (si KLF5) or control SEAP-siRNA (si cont). mRNA expression was assessed by real-time PCR ($n = 6$). (**h**) Effects of KLF5 on *Cpt1b*, *Ucp3* and *Ucp2* promoter reporter activity in C2C12 cells. Not all statistically significant differences are indicated due to lack of space. Error bars, means ± s.e.m in **a**–**f**; means ± s.d. in **g** and **h**. NS, not significant. $^*P < 0.05$; $^{**}P < 0.01$.

*Klf5*$^{+/-}$ mice fed a high-fat diet did not significantly differ from those of wild-type mice (data not shown), the weights of the livers and epididymal fat pads of *Klf5*$^{+/-}$ mice were lower than those of their wild-type littermates (**Supplementary Fig. 1b,c**). To our surprise, despite the smaller body weight gain, *Klf5*$^{+/-}$ mice ate significantly more food than wild-type mice, irrespective of diet (**Fig. 1a**).

The livers and brown adipose tissue (BAT) of *Klf5*$^{+/-}$ mice showed much milder steatosis than did those of wild-type mice, and, within the epididymal WAT, the average size of adipocytes was significantly smaller in *Klf5*$^{+/-}$ mice than in wild-type mice (**Supplementary Fig. 1d,e**).

Oral glucose tolerance tests indicated that *Klf5*$^{+/-}$ mice were protected from high fat–induced glucose intolerance (**Fig. 1b**). Under fasting conditions, serum insulin abundance was lower, and the glucose-lowering effect of insulin was greater, in *Klf5*$^{+/-}$ mice than in wild-type mice (**Fig. 1b**), which suggests that *Klf5*$^{+/-}$ mice are protected from high-fat diet–induced insulin resistance.

Although levels of triglyceride and nonesterified fatty acid were unchanged, serum cholesterol was lower than control levels in *Klf5*$^{+/-}$ mice on a high-fat diet (**Supplementary Fig. 2a** online). Decreased cholesterol synthesis and increased sterol secretion seem to be two major mechanisms by which serum cholesterol abundance was reduced in *Klf5*$^{+/-}$ mice (**Supplementary Fig. 2b**). Because *Klf5* expression is undetectable in the liver, changes in the expression of the genes involved in cholesterol metabolism are probably secondary effects of the systemic metabolic changes.



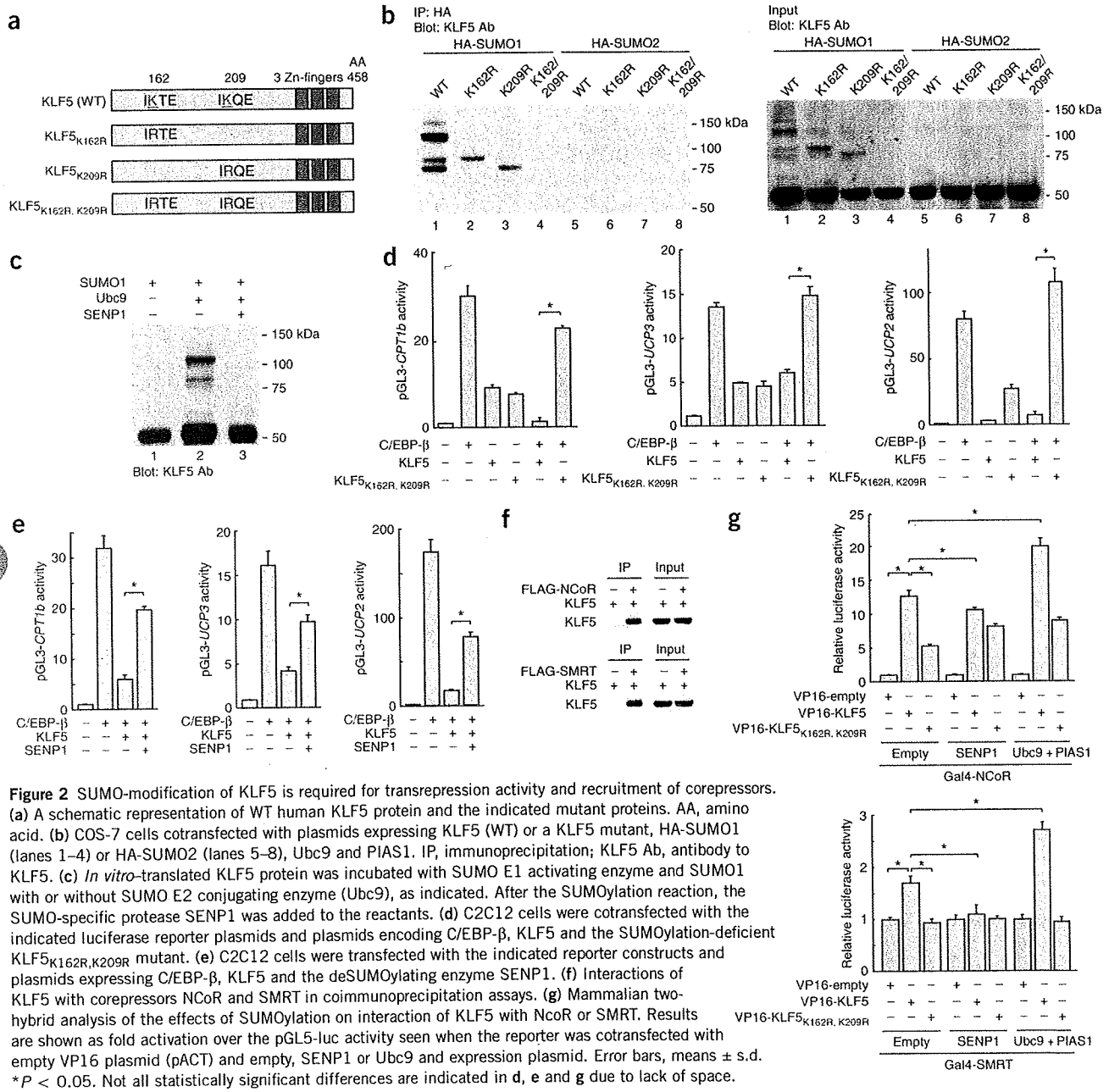


**Figure 2** SUMO-modification of KLF5 is required for transrepression activity and recruitment of corepressors. (**a**) A schematic representation of WT human KLF5 protein and the indicated mutant proteins. AA, amino acid. (**b**) COS-7 cells cotransfected with plasmids expressing KLF5 (WT) or a KLF5 mutant, HA-SUMO1 (lanes 1–4) or HA-SUMO2 (lanes 5–8), Ubc9 and PIAS1. IP, immunoprecipitation; KLF5 Ab, antibody to KLF5. (**c**) *In vitro*–translated KLF5 protein was incubated with SUMO E1 activating enzyme and SUMO1 with or without SUMO E2 conjugating enzyme (Ubc9), as indicated. After the SUMOylation reaction, the SUMO-specific protease SENP1 was added to the reactants. (**d**) C2C12 cells were cotransfected with the indicated luciferase reporter plasmids and plasmids encoding C/EBP-β, KLF5 and the SUMOylation-deficient KLF5$_{K162R,K209R}$ mutant. (**e**) C2C12 cells were transfected with the indicated reporter constructs and plasmids expressing C/EBP-β, KLF5 and the deSUMOylating enzyme SENP1. (**f**) Interactions of KLF5 with corepressors NCoR and SMRT in coimmunoprecipitation assays. (**g**) Mammalian two-hybrid analysis of the effects of SUMOylation on interaction of KLF5 with NcoR or SMRT. Results are shown as fold activation over the pGL5-luc activity seen when the reporter was cotransfected with empty VP16 plasmid (pACT) and empty, SENP1 or Ubc9 and expression plasmid. Error bars, means ± s.d. *$P < 0.05$. Not all statistically significant differences are indicated in **d**, **e** and **g** due to lack of space.

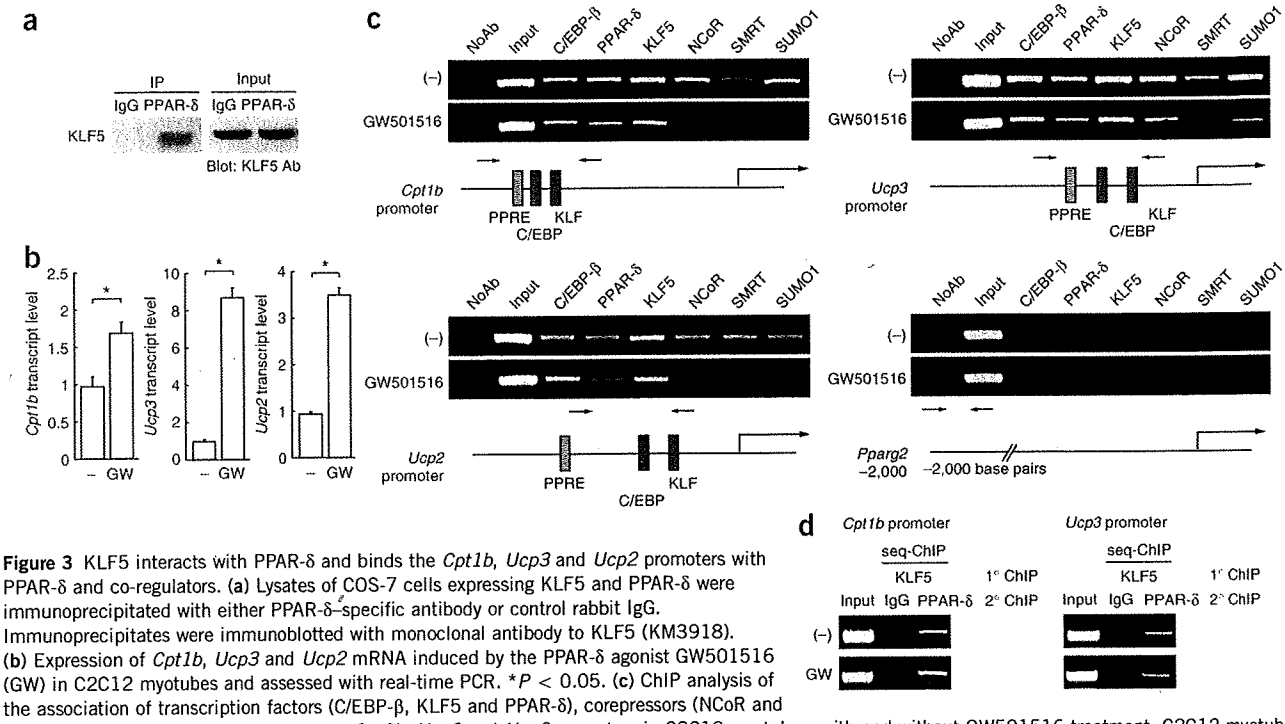


**Figure 3** KLF5 interacts with PPAR-δ and binds the *Cpt1b*, *Ucp3* and *Ucp2* promoters with PPAR-δ and co-regulators. (**a**) Lysates of COS-7 cells expressing KLF5 and PPAR-δ were immunoprecipitated with either PPAR-δ–specific antibody or control rabbit IgG. Immunoprecipitates were immunoblotted with monoclonal antibody to KLF5 (KM3918). (**b**) Expression of *Cpt1b*, *Ucp3* and *Ucp2* mRNA induced by the PPAR-δ agonist GW501516 (GW) in C2C12 myotubes and assessed with real-time PCR. $^*P < 0.05$. (**c**) ChIP analysis of the association of transcription factors (C/EBP-β, KLF5 and PPAR-δ), corepressors (NCoR and SMRT) and SUMO1 with the endogenous *Cpt1b*, *Ucp3* and *Ucp2* promoters in C2C12 myotubes, with and without GW501516 treatment. C2C12 myotubes were fixed in formaldehyde after a 4-h incubation with or without GW501516, after which chromatin samples were prepared for ChIP analysis with the indicated antibodies at top or no antibody (No Ab). The binding motifs of KLF5 (KLF), PPAR-δ (PPRE) and C/EBP-β (C/EBP), as well as the positions of PCR primers (arrows), are shown schematically. A PCR primer set that amplified a region 2,000 base pairs 5′ of the *Pparg2* transcription start site, which does not contain a KLF, C/EBP or PPRE motif, served as a negative control (*Pparg2* –2,000). (**d**) Sequential ChIP analysis of the simultaneous association of KLF5 and PPAR-δ. Chromatin samples were subjected to sequential immunoprecipitation with antibodies to KLF5 and PPAR-δ.



Serum leptin abundance was significantly lower and serum adiponectin abundance was significantly higher in the *Klf5*$^{+/-}$ mice than in wild-type control mice (**Supplementary Fig. 2a**). Moreover, *Klf5*$^{+/-}$ mice maintained better leptin sensitivity when fed a high-fat diet (**Supplementary Fig. 2c**). Taken together, these findings suggest that *Klf5*$^{+/-}$ mice are protected from high-fat diet–induced obesity and metabolic abnormalities.

### Increased systemic energy expenditure in *Klf5*$^{+/-}$ mice

Although the respiratory exchange ratios were comparable between *Klf5*$^{+/-}$ and wild-type mice (**Supplementary Fig. 2d**), $O_2$ consumption was higher in the former mice (**Fig. 1c**), as was the rectal temperature (wild-type, 37.7 ± 0.13 °C versus *Klf5*$^{+/-}$, 38.6 ± 0.14 °C; $n = 11$ each, $P < 0.05$). This means that the level of systemic energy expenditure was higher in *Klf5*$^{+/-}$ mice. In contrast, spontaneous locomotive activity did not significantly differ between *Klf5*$^{+/-}$ and wild-type mice (**Supplementary Fig. 2e**).

Hyperinsulinemic euglycemic clamp studies showed that the haploinsufficiency of *Klf5* protected against insulin resistance in skeletal muscle, but not in the liver (**Fig. 1d**).

### Upregulation of lipid oxidation genes in *Klf5*$^{+/-}$ mice

Expression of *Klf5* mRNA has been detected in both skeletal muscle and WAT, but not in liver[29,30] or BAT (data not shown). A high-fat diet increased the expression of both *Klf5* mRNA and KLF5 protein in the soleus muscles of wild-type mice (**Fig. 1e** and **Supplementary Fig. 3a** online). In *Klf5*$^{+/-}$ mice, by contrast, not only was *Klf5* expression not significantly upregulated by a high-fat diet, but also its level was about half that seen in the wild-type mice (**Fig. 1e**).

Expression of genes encoding CPT1b and medium chain acyl-CoA dehydrogenase (ACADM), two key rate-limiting enzymes involved in fatty acid oxidation, as well as acyl-CoA oxidase (ACOX1) and UCP2 and UCP3, was significantly higher in soleus muscle from *Klf5*$^{+/-}$ mice than in muscle from wild-type mice (**Fig. 1f**). Although WAT also expresses *Klf5*, the levels of expression of the above-mentioned genes were unchanged in WAT (**Supplementary Fig. 3b**).

### KLF5 directly regulates fatty acid oxidation genes

C2C12 myotubes transfected with *Klf5*-specific short interfering RNA (siRNA) showed significantly greater expression of *Ucp2*, *Ucp3*, *Acox1*, *Cpt1b* and *Acadm* than those transfected with the control soluble alkaline phosphatase (SEAP)-siRNA (**Fig. 1g**), supporting the notion that KLF5 represses expression of these genes in skeletal muscle cells in a cell-autonomous manner.

To analyze the mechanisms by which KLF5 controls those genes, we focused on *Cpt1b*, *Ucp3* and *Ucp2* because the promoter regions of these genes have been shown to contain binding motifs for C/EBP, which interacts with KLF5[28]. As was reported previously[31–34], C/EBP-β strongly transactivated the *Cpt1b*, *Ucp3* and *Ucp2* promoters in reporter assays (**Fig. 1h**). By itself, KLF5 increased the promoter activities moderately; however, addition of KLF5 together with C/EBP-β resulted in strong inhibition of C/EBP-β–mediated transactivation of the promoters (**Fig. 1h**).

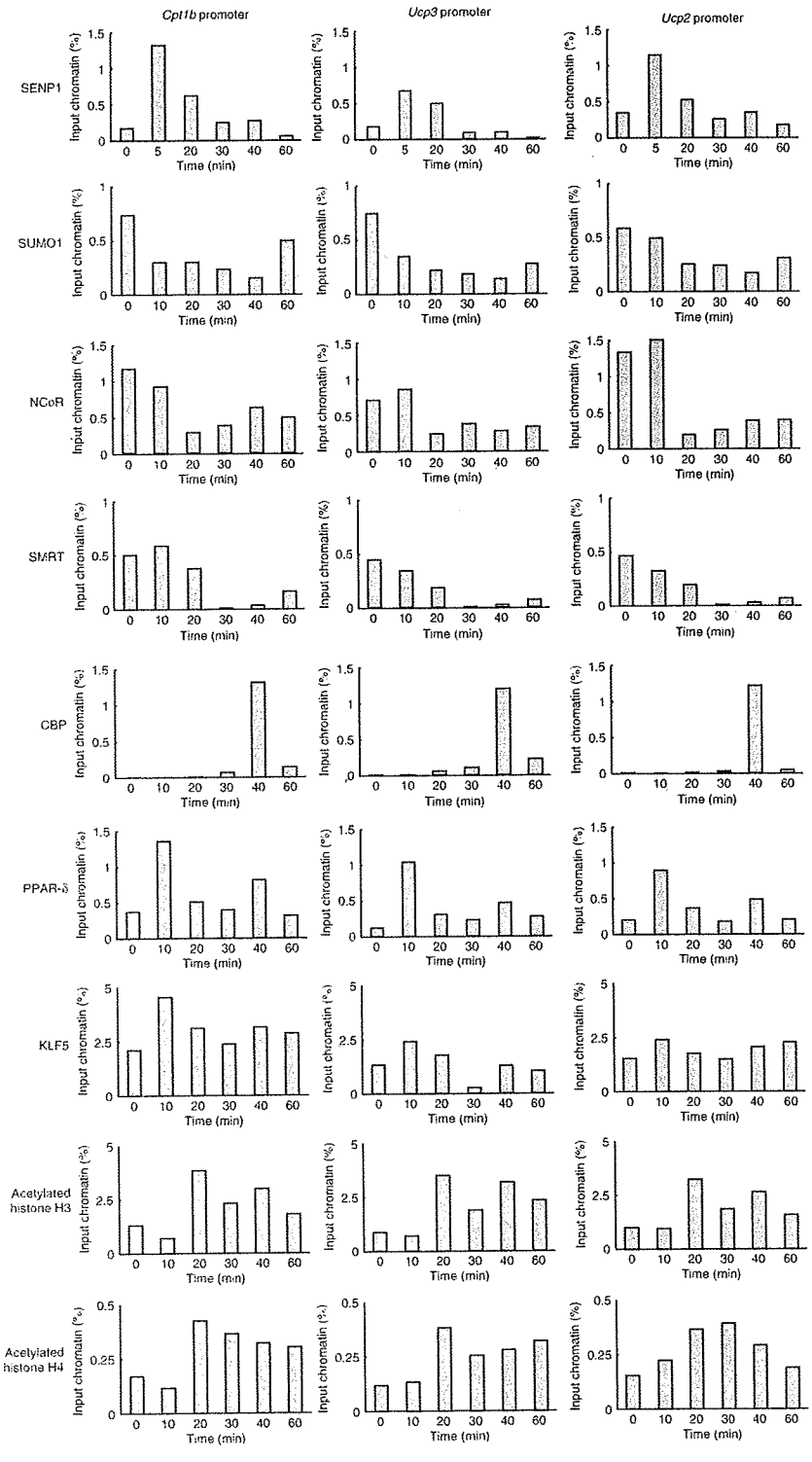


**Figure 4** Dynamic exchange of co-regulators and deSUMOylation induced by GW501516. C2C12 myotubes were treated with 1 μM GW501516 and harvested at the indicated time points. Collected chromatin samples were subjected to ChIP analysis with the specific antibodies indicated at left. The amount of immunoprecipitated *Cpt1b*, *Ucp3* and *Ucp2* promoter region was quantified by real-time PCR with the specific primers indicated in **Figure 3c**. Values are expressed as percentage of input. SENP1 association was analyzed in chromatin samples harvested at 5 min. All ChIPs were performed from a single chromatin preparation for each time point. Data are representative of three independent experiments.

### KLF5 is SUMOylated, which is required for transrepression

The results presented so far suggest that KLF5 directly inhibits expression of genes encoding enzymes involved with fatty acid oxidation. This finding is noteworthy in that, to our knowledge, all of the genes identified to date as direct targets of KLF5 are transactivated by KLF5, with the possible exception of *Klf4* (ref. 35). Recent studies have shown that transcription factors that are post-translationally conjugated with SUMO often inhibit transcription[21]. We found two sites that fit the consensus motif for SUMOylation in human KLF5; the lysines are at amino acid positions 162 and 209 (**Fig. 2a**). The SUMOylation motifs containing those lysines are fully conserved in mouse, rat and human KLF5.

We then tested whether the potential SUMO-targeted lysines could be SUMOylated. Plasmids encoding wild-type KLF5 and hemagglutinin (HA)-tagged SUMO1 were transfected into COS-7 cells. Three major bands containing KLF5 (~85 kDa, ~95 kDa and ~120 kDa) were detected in the immunoprecipitates pulled down with an antibody to HA, indicating that there are three major forms of SUMOylated KLF5 (**Fig. 2b**). The most slowly migrating form, with an apparent molecular weight of 120 kDa, was the most abundant (**Fig. 2b**). A KLF5 mutant in which Lys162 was replaced with an arginine ($KLF5_{K162R}$) produced a single band at 95 kDa, whereas a mutant in which Lys209 was replaced with arginine ($KLF5_{K209R}$) produced an 85-kDa band (**Fig. 2b**). The $KLF5_{K162R,K209R}$ double mutant produced no SUMOylated KLF5 protein (**Fig. 2b**). These results indicate that two lysines, Lys162 and Lys209, can be ligated with SUMO1. In contrast to SUMO1, SUMO2 was a poor modifier of KLF5 (**Fig. 2b**), and, given that SUMO2 and SUMO3 are closely related to each other[36,37], we suggest that KLF5 is a substrate for modification with SUMO1 only. To further test this idea, we performed an *in vitro* SUMOylation assay and found that KLF5 was SUMOylated when incubated with SUMO1, E1 activating enzyme and the SUMO-conjugating enzyme Ubc9 (**Fig. 2c**). The deSUMOylating enzyme SENP1 efficiently removed SUMO1 from KLF5 (**Fig. 2c**).

To analyze the effects of SUMOylation on the function of KLF5, we next cotransfected C2C12 myotubes with *CPT1b*, *UCP3* and *UCP2* promoter reporter plasmids along with either wild-type KLF5 or the SUMOylation-deficient mutant $KLF5_{K162R,K209R}$. Whereas the wild-type KLF5 strongly

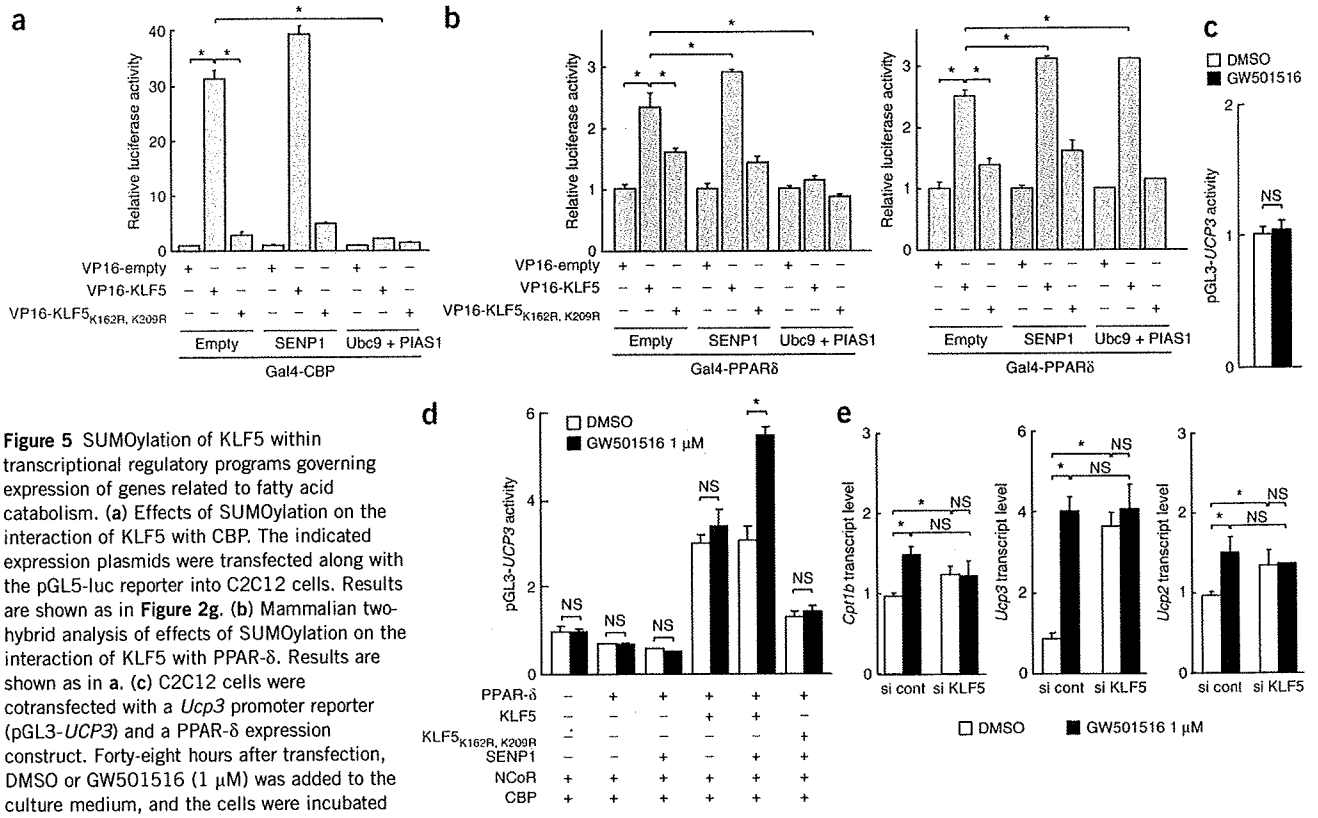


**Figure 5** SUMOylation of KLF5 within transcriptional regulatory programs governing expression of genes related to fatty acid catabolism. (**a**) Effects of SUMOylation on the interaction of KLF5 with CBP. The indicated expression plasmids were transfected along with the pGL5-luc reporter into C2C12 cells. Results are shown as in **Figure 2g**. (**b**) Mammalian two-hybrid analysis of effects of SUMOylation on the interaction of KLF5 with PPAR-δ. Results are shown as in **a**. (**c**) C2C12 cells were cotransfected with a *Ucp3* promoter reporter (pGL3-*UCP3*) and a PPAR-δ expression construct. Forty-eight hours after transfection, DMSO or GW501516 (1 μM) was added to the culture medium, and the cells were incubated for an additional 5 h. (**d**) The pGL3-*UCP3* reporter plasmid was cotransfected with the indicated combinations of expression plasmids and then treated with DMSO or GW501516 as in **c**. The luciferase activity was normalized to the activity in the cells transfected with plasmids encoding CBP and NCoR and treated with DMSO. (**e**) C2C12 myotubes were transfected with siRNA, and 40 h later the cells were treated with either GW501516 or DMSO and cultured for an additional 3 h. mRNA expression levels were normalized with respect to the levels in cells transfected with control siRNA and treated with DMSO ($n = 3$). Error bars, means ± s.d. $^*P < 0.05$. Not all statistically significant differences are indicated in **a**, **b**, **d** and **e** due to lack of space.



inhibited the transactivation of promoter activity of *Cpt1b*, *Ucp3* and *Ucp2* by C/EBP-β, the KLF5K162/209R mutant did not, suggesting that SUMOylation of Lys162 and Lys209 is essential for transrepression of promoter activity by KLF5 (**Fig. 2d**). This finding was confirmed by cotransfecting a plasmid encoding the deSUMOylating enzyme SENP1, which reversed the repression of promoter activity by KLF5 (**Fig. 2e**). Thus, SUMOylation of KLF5 seems to be essential for its transrepressive activity on the *Cpt1b*, *Ucp3* and *Ucp2* promoters.

### KLF5 interacts with corepressors NCoR and SMRT

Previous studies have shown that SUMOylation of the transcription factors PPAR-γ and KLF3 increased their affinity for the corepressors NCoR and SMRT[22,38]. We found that NCoR and SMRT specifically bound KLF5 in coimmunoprecipitation assays (**Fig. 2f**). In addition, wild-type KLF5 and NcoR or SMRT interacted in mammalian two-hybrid assays (**Fig. 2g**). By contrast, the unSUMOylatable VP16-KLF5$_{K162R,K209R}$ construct showed a significantly lower degree of interaction with Gal4-NcoR and no interaction with Gal4-SMRT (**Fig. 2g**). The reporter activities indicating the interactions between KLF5 and NcoR or SMRT were significantly diminished when deSUMOylation was promoted by overexpression of SENP1; conversely, the reporter activities were significantly augmented when SUMOylation was promoted by Ubc9 and PIAS1 overexpression (**Fig. 2g**). Collectively, these findings show that SUMOylation of KLF5 is key for its interactions with NcoR and SMRT.

Another possible mechanism by which SUMOylation could inhibit transcriptional activity is through inhibition of DNA binding[39]. However, DNA affinity binding assays showed that SUMOylated KLF5, as well as unSUMOylated KLF5, could bind target oligomeric DNA (**Supplementary Fig. 4** online).

### KLF5, PPAR-δ and corepressors bind endogenous promoters

We next investigated the role of KLF5 and its SUMOylation in transcriptional programs regulating energy metabolism and its interplay with other regulatory molecules. We noticed a striking similarity between the metabolic phenotypes of *Klf5*$^{+/-}$ mice and those of mice treated with the PPAR-δ–specific agonist GW501516[14], which has been shown to induce expression of *Cpt1b*, *Ucp3* and *Ucp2* in skeletal muscle[13–15]. The promoters of these genes contain potential PPAR binding sites[31–33], and coimmunoprecipitation assays showed that KLF5 is capable of physically associating with PPAR-δ (**Fig. 3a**). On the basis of these findings, we hypothesized that KLF5 controls expression of genes involved in energy metabolism by working within transcriptional regulatory complexes, where it interacts with PPAR-δ, NcoR and SMRT.

To test this notion, we asked whether KLF5, PPARδ, NCoR and SMRT associates with the endogenous *Cpt1b*, *Ucp3* and *Ucp2* promoters and whether this association could be modulated by GW501516. Chromatin samples were prepared from C2C12 myotubes incubated for 4 h with GW501516 and subjected to chromatin

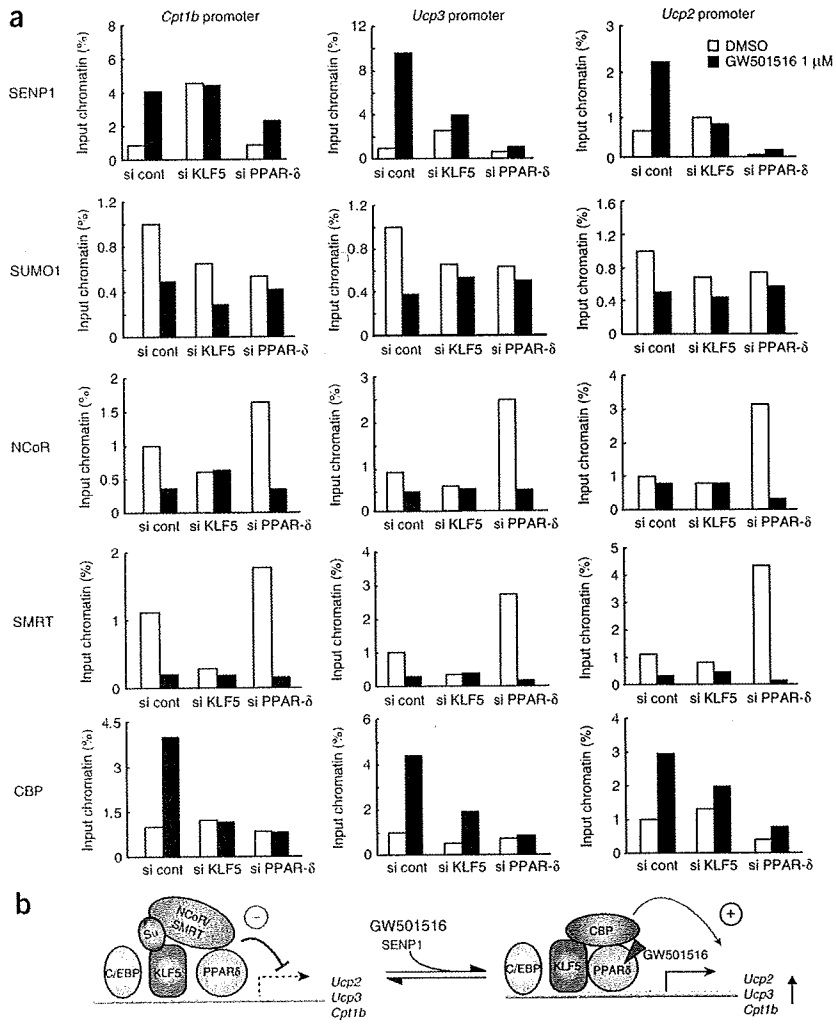


**Figure 6** KLF5 has an essential role in the formation of transcriptional regulatory complexes that respond to GW501516 action on the target gene promoters. (**a**) C2C12 myotubes were transfected with siRNAs for *Klf5* and *Ppard* (si PPAR-δ). After 40 h, the cells were incubated with GW501516 or DMSO for an additional 5 min (SENP1) or 40 min (SUMO1, NCoR, SMRT and CBP) and harvested for ChIP analyses. The amount of immunoprecipitated *Cpt1b*, *Ucp3* and *Ucp2* promoter region was quantified by real-time PCR. Values are expressed as percentage of input. Knocking down *Klf5* resulted in decreased association of NCoR and SMRT with the promoters at baseline and decreased GW501516-induced association with CBP. All ChIPs were performed from a single chromatin preparation for each setting. (**b**) A model of the transcriptional regulatory programs governing expression of *Cpt1b*, *Ucp3* and *Ucp2* in skeletal muscle, indicating that under basal conditions, SUMOylated KLF5 and unliganded PPAR-δ interact with the corepressors NcoR and SMRT to form transcriptionally repressive complexes. GW501516, however, initiates rapid local deSUMOylation that is followed by an exchange of co-regulators, chromatin remodeling and activation of transcription. In transcriptionally active complexes, unSUMOylated KLF5 interacts with CBP and liganded PPAR-δ.



immunoprecipitation (ChIP) assays. GW501516 treatment increased expression of all three genes (**Fig. 3b**). ChIP analyses showed that under basal conditions, C/EBP-β, KLF5, PPAR-δ, NCoR and SMRT all associated with the endogenous promoters (**Fig. 3c**). As expected, SUMO1 also associated with the promoters, indicating that one or more of the bound proteins, which very likely included KLF5, were SUMOylated (**Fig. 3c**). Given the ability of KLF5 to transrepress promoter activity, we anticipated that GW501516 might eliminate KLF5 from the transcriptional regulatory complexes, but to our surprise GW501516 did not significantly affect the association of KLF5 with the promoters (**Fig. 3c**). In contrast, GW501516 clearly inhibited the association of NcoR and SMRT (**Fig. 3c**). The association of SUMO1 was also much reduced (**Fig. 3c**). GW501516 thus seems to reduce the association of SUMOylated proteins to the promoters and to promote an exchange of co-regulators that likely leads to activation of the promoters. Consistent with the notion that GW501516 affects the SUMOylated states of KLF5, the band corresponding to doubly SUMOylated KLF5 found in untreated C2C12 lysates was eliminated by GW501516 treatment (**Supplementary Fig. 5** online).

### PPAR-δ agonist promotes deSUMOylation and transactivation

Unexpectedly, we observed an association between KLF5 and PPAR-δ on both repressed and activated promoters (**Fig. 3c**). Sequential ChIP assays further confirmed that KLF5 and PPAR-δ simultaneously associated with the promoters and that this association was found under both baseline conditions and during GW501516 treatment (**Fig. 3d**). This prompted us to hypothesize that KLF5 and PPAR-δ have different roles within repressive and activating regulatory complexes. To test this possibility, we analyzed the molecular steps leading to promoter activation in more detail by a set of ChIP assays using C2C12 chromatin samples obtained at various time points after liganding PPAR-δ with GW501516. We found that GW501516 treatment induced dynamic alterations in SUMOylation, cofactor binding and histone acetylation on the *Cpt1b*, *Ucp3* and *Ucp2* promoters (**Fig. 4**). It induced rapid and transient recruitment of SENP1 by 5 min after the initiation of treatment (**Fig. 4**). This SENP1 recruitment was followed by a reduction in the association of SUMO1 with the promoter by 10–20 min, suggesting that GW501516 promoted local deSUMOylation of regulatory factors, most likely including KLF5, by recruiting SENP1 (**Fig. 4**). As SUMO1 modification declined, the association of the corepressors NCoR and SMRT also declined, beginning at 20 min (**Fig. 4**). Conversely, the association of the coactivator CBP began increasing at 20 min and peaked at 40 min (**Fig. 4**). Hyperacetylation of histones H3 and H4 was observed beginning at 20 min (**Fig. 4**). Thus, GW501516 treatment promoted local deSUMOylation within 10 min, and this was followed by release of corepressors, recruitment of coactivators and chromatin remodeling, all of which led to transcriptional activation.

KLF5 and PPAR-δ were found to associate with the promoters even under basal conditions in cells not treated with GW501516 (0 min; **Fig. 4**). That SUMO1, NCoR and SMRT were also associated with the promoters at 0 min suggests that KLF5 and unliganded PPAR-δ form

transrepressive complexes on the promoters under basal conditions. GW501516 treatment did not eliminate the association between KLF5 and PPAR-δ and even increased their association somewhat at 10 min (**Fig. 4**). By 20–30 min, however, it had declined to levels similar to those observed at 0 min, but it increased again by 40 min (**Fig. 4**).

### KLF5 SUMOylation toggles associated co-regulators

Our reporter and ChIP analyses showed that SUMOylated KLF5 represses *Cpt1b*, *Ucp3* and *Ucp2* promoter activity, but they also suggest that KLF5 associates with transcriptional activating complexes on the promoters in GW501516-treated cells. We therefore hypothesized that unSUMOylated KLF5 activates the promoters by interacting with appropriate coactivators. Because we found CBP to be associated with activated promoters in our ChIP assays (**Fig. 4**), we first tested this hypothesis by analyzing the interaction between KLF5 and CBP. Mammalian two-hybrid assays showed that KLF5 interacts with CBP and that this interaction requires intact Lys162 and Lys209 residues (**Fig. 5a**). Enhancement of deSUMOylation by overexpression of SENP1 increased the interaction, whereas promotion of SUMOylation by overexpression of Ubc9 and PIAS1 strongly inhibited the interaction (**Fig. 5a**). This inhibitory effect of SUMOylation on the association of CBP with KLF5 is in sharp contrast to the interactions between KLF5 and NcoR or SMRT, which were enhanced by SUMOylation (**Fig. 2g**). SUMOylation may thus toggle the interaction of KLF5 between the coactivator CBP and corepressors NcoR and SMRT.

Mammalian two-hybrid assays showed that KLF5 also interacts with PPAR-δ, that the interaction is dependent on the presence of intact Lys162 and Lys209 residues and that it was strongly inhibited by overexpression of Ubc9 and PIAS1 (**Fig. 5b**). This suggests that SUMOylation of KLF5 inhibits its interaction with PPAR-δ. Notably, treatment with GW501516 completely reversed the inhibitory effect of the overexpression of Ubc9 and PIAS1 on the KLF5–PPAR-δ interaction (**Fig. 5b**), suggesting that liganding PPAR-δ might induce deSUMOylation, thereby increasing the affinity between the two molecules.

### SUMOylation of KLF5 is required for GW501516 response

The results presented so far suggest that KLF5 and PPAR-δ each have dual roles in the transcriptional regulation of *Cpt1b*, *Ucp3* and *Ucp2* promoter activity. Of note, these three promoters were not activated by GW501516 in reporter assays in C2C12 cells when only PPAR-δ was overexpressed (**Fig. 5c** and data not shown). This led us to hypothesize that KLF5 plus its SUMOylation and co-regulators are required for GW501516-dependent transcriptional control. Bearing in mind the results of our earlier ChIP assays, we tested this idea by attempting to recapitulate GW501516-induced deSUMOylation by coexpressing PPAR-δ, KLF5, C/EBP-β, NCoR, CBP and SENP1 with a *Ucp3* promoter reporter (**Supplementary Fig. 6** online). In this setting, GW501516 increased promoter activity, and KLF5 was required for the GW501516-dependent activation (**Supplementary Fig. 6**). To assess the specific roles of the factors involved, we next analyzed various combinations of the factors and found that overexpression of C/EBP-β is dispensable with respect to the GW501516-dependent response (**Fig. 5d** and data not shown). We then analyzed the role of SUMOylation using the combinations of coexpressed factors indicated in **Figure 5d**. When PPAR-δ alone was expressed with NCoR and CBP, no response to GW501516 was observed, and addition of SENP1 did not yield a GW501516 response (**Fig. 5d**). Addition of KLF5 to the combination of PPAR-δ, NCoR and CBP resulted in a modest increase in reporter activity, and although further addition of SENP1 did not alter baseline promoter activity, the activity was now significantly increased by GW501516, confirming that KLF5 is required for GW501516 to elicit a response with this combination of regulatory factors (**Fig. 5d**). Replacement of wild-type KLF5 with $KLF5_{K162R,K209R}$ eliminated the response to GW501516, confirming that SUMOylatable KLF5 is necessary for execution of the transcriptional regulatory programs. These results show that KLF5 is essential for GW501516-dependent transcriptional regulation of *Ucp3* promoter activity and that the SUMOylation state of KLF5 is probably a key determinant in that control.

To further analyze the role of KLF5 in the control of endogenous target genes, we knocked down *Klf5* expression in C2C12 myotubes (**Fig. 5e**). As shown previously in **Figure 1g**, knockdown of *Klf5* led to increased expression of *Cpt1b*, *Ucp2* and *Ucp3*. Treatment with GW501516 did not significantly increase expression of these genes in the *Klf5* knockdown cells (**Fig. 6a**). KLF5 thus seems to be crucial for GW501516-mediated induction of these genes. In addition, knocking down *Ubc9* and *Pias1* led to increases in *Cpt1b*, *Ucp2* and *Ucp3* expression under both baseline and GW501516-treated conditions, indicating that Ubc9 and PIAS1 are crucial in the transcriptional regulation of these genes, presumably via control of SUMOylation (**Supplementary Fig. 7** online).

To gain further insight into the roles of KLF5 and PPAR-δ in the formation of repressive and activating transcriptional complexes, we knocked down these transcription factors in C2C12 myotubes, after which we subjected the cells to ChIP analyses. Knocking down *Klf5* reduced the association of SUMO1, NCoR and SMRT with the promoter in the GW501516-untreated cells, indicating that KLF5 is required for the formation of transcriptionally repressive complexes (**Fig. 6a**). In contrast, the recruitment of CBP induced by GW501516 was also clearly repressed in *Klf5*-knockdown cells, suggesting that KLF5 is also required for activation of the promoters (**Fig. 6a**). Knockdown of *Ppard* led to increases in the association of NCoR and SMRT with the target *Cpt1b*, *Ucp2* and *Ucp3* promoters under baseline conditions, and GW501516-induced CBP recruitment was also inhibited by *Ppard* knockdown (**Fig. 6a**), suggesting that KLF5 and PPAR-δ play differential parts in the formation of transcriptional regulatory complexes.

## DISCUSSION

We have found that haploinsufficiency of *Klf5* protects mice from high-fat diet–induced obesity and insulin resistance, particularly in skeletal muscle, and that enhanced systemic energy expenditure is a key mechanism underlying the metabolic phenotypes in $Klf5^{+/-}$ mice (**Fig. 1**). Knocking down *Klf5* in the skeletal muscle ($Klf5^{+/-}$) and in C2C12 myotubes upregulated expression of several genes involved in fatty acid oxidation and energy uncoupling, including *Cpt1b*, *Acadm*, *Acox1*, *Ucp2* and *Ucp3* (**Fig. 1f,g**). CPT1b is the rate-limiting enzyme catalyzing fatty acid import into mitochondria for β-oxidation[40]. Its overexpression reportedly protects cultured myotubes from fatty acid–induced insulin resistance[41], and its pharmacological inhibition leads to insulin resistance in rats[42]. Although the results of our study and a number of earlier studies have shown that expression of *Ucp2* and *Ucp3* mRNA is coordinately regulated in skeletal muscle, the main uncoupling protein expressed in skeletal muscle is reportedly UCP3[33]. Although the effect of *Ucp3* ablation on obesity is unclear in mice[43], overexpression of UCP3 increases fatty acid oxidation and protects against high-fat diet–induced obesity and insulin resistance[44,45]. Taken together, the observed reduction in high-fat diet–induced obesity and insulin resistance and the enhanced energy expenditure in $Klf5^{+/-}$ mice probably reflect, at least in part, a coordinated alteration of the

expression of genes involved in fatty acid metabolism caused by the haploinsufficiency of *Klf5*. Although we focused on *Cpt1b*, *Ucp3* and *Ucp2* in the present study, it is very likely that expression of other genes (for example, *Acox1* and *Acadm*) also is controlled by transcriptional programs involving KLF5 and also contributes to the metabolic phenotypes in $Klf5^{+/-}$ mice.

SUMOylation is now considered to be a major regulatory modification leading to repression of transcription[21]. Our results show that SUMOylation is a key modulator of transcriptional regulatory programs governing fatty acid metabolism, in part because SUMOylation of KLF5 increases its affinity for NCoR and SMRT (**Fig. 2g**) while decreasing its affinity for CBP and PPARδ (**Fig. 5a,b**). This change in interacting co-regulators induced by SUMOylation apparently enables KLF5 to have dual roles in transcriptional regulation. SUMOylation thus seems to serve as a molecular switching mechanism controlling fatty acid metabolism in response to cellular and environmental cues.

Our ChIP analyses clearly showed that GW501516 induces dynamic changes in the assembly of transcriptional regulatory complexes, chromatin structure and SUMO-modification of factors binding to endogenous *Cpt1b*, *Ucp2* and *Ucp3* promoters (**Fig. 4**). Of note, SENP1 was recruited within 5 min after GW501516 treatment, leading to dissociation of SUMO1 from the promoter within 10 min. This rapid local deSUMOylation was followed by dissociation of the corepressors NCoR and SMRT, increased association of CBP and hyperacetylation of histones on the promoters. Thus, liganding of PPAR-δ seems to induce rapid local deSUMOylation and exchange of the components of transcriptional regulatory complexes and chromatin remodeling. On the basis of these findings and our data on the interactions between KLF5, PPAR-δ and their co-regulators, we propose the following model of transcriptional regulation of *Cpt1b*, *Ucp2* and *Ucp3* promoter activity (**Fig. 6b**). Under basal conditions, SUMOylated KLF5 is associated with NCoR and SMRT and functions to repress transcription. Because mammalian two-hybrid assays indicate that SUMOylated KLF5 has a low affinity for PPAR-δ, it is unlikely that it directly associates with unliganded PPAR-δ. Instead, the findings that unliganded PPAR-δ interacts with NCoR and SMRT[18,19] suggest these two co-regulators mediate the interaction between KLF5 and unliganded PPAR-δ to form transcriptionally repressive complexes. Upon GW501516 treatment, liganded PPAR-δ recruits SENP1 and promotes local deSUMOylation. Release of SUMO1 from KLF5 increases its affinity for PPAR-δ and CBP, leading to formation of transcriptional activating complexes. C/EBP-β seems to be a component of transcriptional activating complexes and is probably required for promoter transactivation. However, its precise regulatory function is not immediately clear.

The model depicted in **Figure 6b** predicts that KLF5 and its SUMOylation are integral to GW501516-dependent transactivation of PPAR-δ targets. As expected, PPAR-δ required KLF5, SENP1 and various co-regulators to activate the *Ucp2*, *Ucp3* and *Cpt1b* promoters in response to GW501516 (**Fig. 5d**). The fact that SUMOylation-deficient $KLF5_{K162R,K209R}$ was not capable of supporting GW501516-dependent activation highlights the importance of the SUMOylation state of KLF5 in determining its interaction with co-regulators and with PPAR-δ within transcriptional regulatory complexes. Moreover, whereas knockdown of *Klf5* resulted in increased baseline *Cpt1b*, *Ucp2* and *Ucp3* expression, it reduced GW501516-mediated induction of the genes (**Fig. 5e**). And although association of SUMO1, NCoR and SMRT with the target promoters was reduced in *Klf5*-knockdown cells under baseline conditions, recruitment of CBP induced by GW501516 was also reduced (**Fig. 6a**). These findings support a model in which KLF5 is required for the formation of both repressive and activating complexes (**Fig. 6b**). The finding that the association of corepressors with the *Cpt1b*, *Ucp2* and *Ucp3* promoters was reduced by *Klf5* knockdown also suggests that the increased expression of these genes observed in $Klf5^{+/-}$ skeletal muscle probably reflects derepression of the genes due to *Klf5* haploinsufficiency.

Our ChIP analyses showed that proteins associated with the *Ucp2*, *Ucp3* and *Cpt1b* promoters are SUMOylated under basal conditions (**Fig. 4**). However, current ChIP methods do not enable identification of a single protein that has a specific modification; instead, because formaldehyde crosslinks macromolecular complexes nonspecifically, they can only report that a modification exits within a protein complex. Nonetheless, given our findings that KLF5 can be SUMOylated (**Fig. 2**), that SUMOylated KLF5 interacts with NCoR and SMRT (**Fig. 2g**), which are also associated with repressive promoters, and that endogenous levels of SUMOylated KLF5 in C2C12 myotubes were diminished by GW501516 treatment (**Supplementary Fig. 5**), it seems very likely that KLF5 was among the SUMOylated proteins detected in the ChIP assays on the repressed promoters. That said, it is also possible that other molecules other than KLF5 are also SUMOylated. It would be useful to know whether SUMOylation of other molecules, including PPAR-δ, is involved in the transcriptional regulation of fatty acid metabolism.

Transient recruitment of SENP1 to the GW501516-treated promoters and the subsequent disassociation of SUMO1 from the promoters strongly suggests that deSUMOylation takes place locally. However, the findings that the amount of associated KLF5 and PPAR-δ was altered by GW501516 also suggest the possibility that unSUMOylated KLF5 was recruited to the promoters to replace SUMOylated KLF5. Consistent with this possibility, it is known that molecules within transcriptional regulatory complexes are dynamically exchanged during transcriptional activation, which may involve protein degradation[46]. Although the precise molecular events will need to be clarified in future studies, our ChIP results clearly indicate that GW501516 induces ordered and sequential protein modifications and exchanges including deSUMOylation, exchange of co-regulators and chromatin remodeling.

Because a growing body of evidence indicates that PPAR-δ is a key transcription factor governing fatty acid metabolism, PPAR-δ is now considered to be an attractive target for the development of therapeutic strategies against metabolic syndrome[15,19,47,48]. However, PPAR-δ is widely expressed in tissues other than skeletal muscle and so may have a variety of tissue-specific functions. As a consequence, strategies focusing on PPAR-δ need to be carefully evaluated for possible side effects[47]. Efforts are now underway to develop ligands for nuclear receptors that activate only a subset of the functions activated by the cognate ligand, or that act in a cell type–selective manner. Unlike PPAR-δ, KLF5 is not expressed in the liver, suggesting that further elucidation of the transcriptional regulator programs involving PPAR-δ and KLF5 could potentially lead to development of such selective ligands.

In conclusion, we have shown that KLF5 is a key component of lipid metabolism in skeletal muscle and that SUMOylation of KLF5 functions as a molecular switch for fatty acid oxidation programs involving PPAR-δ and various co-regulators.

## METHODS

**Mice.** *Klf5*-knockout heterozygous mice ($Klf5^{+/-}$) were generated as previously described[44]. We backcrossed the founder mice with C57/BL6J mice at least seven times. We used wild-type littermates as controls throughout the study. We fed mice either a standard chow that had a 4.6% (w/w) fat content or a

high-fat diet that had a 32% (w/w) fat and 6.75 % (w/w) sucrose content (Crea). We fed mice the high-fat diet for 12 weeks, beginning at 4 weeks of age. All experiments were approved by the University of Tokyo Ethics Committee for Animal Experiments and strictly adhered to the guidelines for animal experiments of the University of Tokyo.

**Small interfering RNA.** We generated siRNAs with a Silencer siRNA construction kit (Ambion) according to the manufacturer's protocols for the experiments shown in **Figure 1g**. The siRNA sequences for *Klf5* were reported previously[28]. For the experiments in **Figures 5e** and **6a**, we purchased siRNAs for *Klf5*, *Ppard* and control (ON-TARGET plus SMART pool) from Dharmacon. We transfected fully differentiated C2C12 myotubes grown in a 6-cm dish with 280 ng of double-stranded siRNA using a Deliver X kit (Veritas) according to the manufacturer's instructions. Forty-eight hours later, we harvested the cells for real-time PCR analysis or ChIP analysis.

**KLF5 antibody.** Monoclonal mouse KLF5-specific antibody (KM3918) was raised against the polypeptide CIPEHKKYRRDSASV. We thoroughly analyzed the specificity of this antibody by western blotting and immunohistochemical analyses (data not shown).

**Mammalian two-hybrid assays.** We fused cDNAs encoding full-length wild-type KLF5 and the SUMOylation site mutant $KLF5_{K162R,K209R}$ to the VP16 activation domain in pACT (Promega) to generate VP16-KLF5 and VP16-$KLF5_{K162R,K209R}$. We fused the full-length NCoR cDNA to the Gal4 DNA binding domain in pBIND (Promega) to generate Gal4-NCoR. We transfected the constructs into C2C12 cells with Polyfect transfection reagent (Qiagen). We measured luciferase activity in whole cell lysates 48 h after transfection. For GW501516 treatment, beginning 48 h after transfection, we incubated the cells with or without 1 μM GW501516 for an additional 5 h before harvesting them.

**SUMOylation assay.** To analyze SUMOylation within cells, we used Lipofectamine 2000 to transfect COS-7 cells with plasmids encoding wild-type KLF5 or a SUMOylation site mutant, along with HA-tagged SUMO1, Ubc9 and PIAS1 (Invitrogen). We then immunoprecipitated cell lysates with an HA-specific affinity matrix gel (Roche), after which we washed the immunoprecipitate in lysis buffer (50 mM Tris-Cl pH 7.5, 150 mM NaCl, 0.1% Triton X-100, 1 mM DTT, 10% glycerol, 10 mM EDTA), resolved the proteins by SDS-PAGE and immunoblotted with monoclonal KLF5-specific antibody (KM3918).

For *in vitro* SUMOylation assays, we generated KLF5 protein by *in vitro* translation with a TNT-T7 quick coupled reticulocyte lysate system (Promega). We then subjected a 1.5-μl aliquot of translation product to *in vitro* SUMOylation assays with a SUMOylation kit (BIOMOL) according to the manufacturer's protocols.

**Chromatin immunoprecipitation assay.** We carried out ChIP assays as previously described[28]. For quantitative analysis of the abundance of targeted genomic regions in immunoprecipitates, we determined the levels of the targeted sequences by real-time PCR and normalized them to the levels in untreated control samples[26,27]. We used antibodies to C/EBP-β, PPAR-δ, NCoR (all from Santa Cruz), SMRT (Upstate), SUMO1 (Zymed) and SENP1 (Abgent). For sequential ChIP assays, we immunoprecipitated cross-linked chromatin samples with KLF5-specific antibody, after which we eluted the precipitates and subjected them to another round of ChIP using PPAR-δ–specific antibody. The sequences of the PCR primers are available in the **Supplementary Methods** online.

**Statistical analyses.** We analyzed differences in the body weight change by two-way ANOVA. Luciferase and mammalian two-hybrid assays and gene expression measured by real-time PCR were compared with one-way ANOVA followed by a *post hoc* Tukey-Kramer test for multiple groups, and comparisons between two groups were made with Student's *t*-test. We considered $P$ values $<0.05$ as significant.

*Note: Supplementary information is available on the Nature Medicine website.*

ACKNOWLEDGMENTS

We gratefully acknowledge N. Yamanaka, M. Hayashi, Y. Tani and E. Magoshi for their excellent technical assistance. We thank M. Yamada (Gunma University) for providing pGL3-*UCP2*, C. Glass (University of California, San Diego) for providing FLAG-tagged cDNA encoding mouse NCoR, R. Evans (Salk Institute for Biological Studies) for providing cDNA encoding human SMRT and the Gal4-SMRT expression construct, R. Hay (University of Dundee) for providing pcDNA3-HA-SUMO1 and pcDNA3-HA-SUMO2, E. Yeh (University of Texas–Houston Health Science) for providing pcDNA3-SENP1, and P. Grimaldi (Universite de Nice-Sophia Antipolis) for providing pcDNA3-PPARδ. This study was supported in part by grants-in-aid from the Ministry of Education, Culture, Sports, Science and Technology, Japan (to R.N., I.M. and Y.O.), a research grant from the National Institute of Biomedical Innovation, Japan and Special Coordination Funds for Promoting Science and Technology from Japan Science and Technology Agency (to R.N.), and research grants from Japan Science and Technology Agency, NOVARTIS Foundation for the Promotion of Science, Kato Memorial Bioscience Foundation, Takeda Science Foundation, Cell Science Research Foundation and Tokyo Biochemical Research Foundation (to I.M.).

AUTHOR CONTRIBUTIONS

Y.O. developed the project, performed most of the experiments and data analysis and wrote the manuscript. I.M. developed and supervised the project, designed experiments, performed data analysis and wrote the manuscript. M.O., T. Kubota. and N.K. contributed to the mouse physiology studies. K.F. and K.M. contributed to the *in vitro* studies. K.T. and T. Kadowaki supervised the project and reviewed the manuscript. R.N. directed the project and reviewed the manuscript.

Published online at http://www.nature.com/naturemedicine/
Reprints and permissions information is available online at http://npg.nature.com/reprintsandpermissions/

1. Lowell, B.B. & Spiegelman, B.M. Towards a molecular understanding of adaptive thermogenesis. *Nature* **404**, 652–660 (2000).
2. Weigle, D.S. Appetite and the regulation of body composition. *FASEB J.* **8**, 302–310 (1994).
3. Smith, A.G. & Muscat, G.E. Skeletal muscle and nuclear hormone receptors: implications for cardiovascular and metabolic disease. *Int. J. Biochem. Cell Biol.* **37**, 2047–2063 (2005).
4. Ukropcova, B. *et al.* Dynamic changes in fat oxidation in human primary myocytes mirror metabolic characteristics of the donor. *J. Clin. Invest.* **115**, 1934–1941 (2005).
5. Kelley, D.E. Skeletal muscle fat oxidation: timing and flexibility are everything. *J. Clin. Invest.* **115**, 1699–1702 (2005).
6. Spiegelman, B.M. & Heinrich, R. Biological control through regulated transcriptional coactivators. *Cell* **119**, 157–167 (2004).
7. Lin, J., Handschin, C. & Spiegelman, B.M. Metabolic control through the PGC-1 family of transcription coactivators. *Cell Metab.* **1**, 361–370 (2005).
8. Rawson, R.B. The SREBP pathway. *Nat. Rev. Mol. Cell Biol.* **4**, 631–640 (2003).
9. Evans, R.M., Barish, G.D. & Wang, Y.X. PPARs and the complex journey to obesity. *Nat. Med.* **10**, 355–361 (2004).
10. Mootha, V.K. *et al.* Errα and Gabpa/b specify PGC-1α–dependent oxidative phosphorylation gene expression that is altered in diabetic muscle. *Proc. Natl. Acad. Sci. USA* **101**, 6570–6575 (2004).
11. Wolfrum, C., Asilmaz, E., Luca, E., Friedman, J.M. & Stoffel, M. Foxa2 regulates lipid metabolism and ketogenesis in the liver during fasting and in diabetes. *Nature* **432**, 1027–1032 (2004).
12. Schuler, M. *et al.* PGC1α expression is controlled in skeletal muscles by PPARβ, whose ablation results in fiber-type switching, obesity, and type 2 diabetes. *Cell Metab.* **4**, 407–414 (2006).
13. Dressel, U. *et al.* The peroxisome proliferator–activated receptor β/δ agonist, GW501516, regulates the expression of genes involved in lipid catabolism and energy uncoupling in skeletal muscle cells. *Mol. Endocrinol.* **17**, 2477–2493 (2003).
14. Tanaka, T. *et al.* Activation of peroxisome proliferator–activated receptor δ induces fatty acid β-oxidation in skeletal muscle and attenuates metabolic syndrome. *Proc. Natl. Acad. Sci. USA* **100**, 15924–15929 (2003).
15. Wang, Y.X. *et al.* Peroxisome proliferator–activated receptor δ activates fat metabolism to prevent obesity. *Cell* **113**, 159–170 (2003).
16. Wang, Y.X. *et al.* Regulation of muscle fiber type and running endurance by PPARδ. *PLoS Biol.* **2**, e294 (2004).
17. Lee, C.H. *et al.* Peroxisome proliferator–activated receptor δ promotes very low-density lipoprotein–derived fatty acid catabolism in the macrophage. *Proc. Natl. Acad. Sci. USA* **103**, 2434–2439 (2006).
18. Krogsdam, A.M. *et al.* Nuclear receptor corepressor–dependent repression of peroxisome proliferator–activated receptor δ–mediated transactivation. *Biochem. J.* **363**, 157–165 (2002).
19. Shi, Y., Hon, M. & Evans, R.M. The peroxisome proliferator–activated receptor δ, an integrator of transcriptional repression and nuclear receptor signaling. *Proc. Natl. Acad. Sci. USA* **99**, 2613–2618 (2002).
20. Hay, R.T. SUMO: a history of modification. *Mol. Cell* **18**, 1–12 (2005).
21. Gill, G. Something about SUMO inhibits transcription. *Curr. Opin. Genet. Dev.* **15**, 536–541 (2005).
22. Pascual, G. *et al.* A SUMOylation-dependent pathway mediates transrepression of inflammatory response genes by PPAR-γ. *Nature* **437**, 759–763 (2005).

23. Eaton, E.M. & Sealy, L. Modification of CCAAT/enhancer-binding protein-β by the small ubiquitin-like modifier (SUMO) family members, SUMO-2 and SUMO-3. *J. Biol. Chem.* **278**, 33416–33421 (2003).
24. Hirano, Y., Murata, S., Tanaka, K., Shimizu, M. & Sato, R. Sterol regulatory element-binding proteins are negatively regulated through SUMO-1 modification independent of the ubiquitin/26 S proteasome pathway. *J. Biol. Chem.* **278**, 16809–16819 (2003).
25. Haldar, S.M., Ibrahim, O.A. & Jain, M.K. Kruppel-like factors (KLFs) in muscle biology. *J. Mol. Cell. Cardiol.* **43**, 1–10 (2007).
26. Fujiu, K. *et al.* Synthetic retinoid Am80 suppresses smooth muscle phenotypic modulation and in-stent neointima formation by inhibiting KLF5. *Circ. Res.* **97**, 1132–1141 (2005).
27. Shindo, T. *et al.* Kruppel-like zinc-finger transcription factor KLF5/BTEB2 is a target for angiotensin II signaling and an essential regulator of cardiovascular remodeling. *Nat. Med.* **8**, 856–863 (2002).
28. Oishi, Y. *et al.* Kruppel-like transcription factor KLF5 is a key regulator of adipocyte differentiation. *Cell Metab.* **1**, 27–39 (2005).
29. Shi, H., Zhang, Z., Wang, X., Liu, S. & Teng, C.T. Isolation and characterization of a gene encoding human Kruppel-like factor 5 (IKLF): binding to the CAAT/GT box of the mouse lactoferrin gene promoter. *Nucleic Acids Res.* **27**, 4807–4815 (1999).
30. Watanabe, N. *et al.* BTEB2, a Kruppel-like transcription factor, regulates expression of the SMemb/Nonmuscle myosin heavy chain B (SMemb/NMHC-B) gene. *Circ. Res.* **85**, 182–191 (1999).
31. Brandt, J.M., Djouadi, F. & Kelly, D.P. Fatty acids activate transcription of the muscle carnitine palmitoyltransferase I gene in cardiac myocytes via the peroxisome proliferator–activated receptor α. *J. Biol. Chem.* **273**, 23786–23792 (1998).
32. Medvedev, A.V., Snedden, S.K., Raimbault, S., Ricquier, D. & Collins, S. Transcriptional regulation of the mouse uncoupling protein-2 gene. Double E-box motif is required for peroxisome proliferator–activated receptor-γ–dependent activation. *J. Biol. Chem.* **276**, 10817–10823 (2001).
33. Pecqueur, C. *et al.* Uncoupling protein 2, *in vivo* distribution, induction upon oxidative stress and evidence for translational regulation. *J. Biol. Chem.* **276**, 8705–8712 (2001).
34. van der Leij, F.R. *et al.* Structural and functional genomics of the CPT1B gene for muscle-type carnitine palmitoyltransferase I in mammals. *J. Biol. Chem.* **277**, 26994–27005 (2002).
35. Dang, D.T., Zhao, W., Mahatan, C.S., Geiman, D.E. & Yang, V.W. Opposing effects of Kruppel-like factor 4 (gut-enriched Kruppel-like factor) and Kruppel-like factor 5 (intestinal-enriched Kruppel-like factor) on the promoter of the Kruppel-like factor 4 gene. *Nucleic Acids Res.* **30**, 2736–2741 (2002).
36. Gong, L. & Yeh, E.T. Characterization of a family of nucleolar SUMO-specific proteases with preference for SUMO-2 or SUMO-3. *J. Biol. Chem.* **281**, 15869–15877 (2006).
37. Tatham, M.H. *et al.* Polymeric chains of SUMO-2 and SUMO-3 are conjugated to protein substrates by SAE1/SAE2 and Ubc9. *J. Biol. Chem.* **276**, 35368–35374 (2001).
38. Perdomo, J., Verger, A., Turner, J. & Crossley, M. Role for SUMO modification in facilitating transcriptional repression by BKLF. *Mol. Cell. Biol.* **25**, 1549–1559 (2005).
39. Chou, C.C. *et al.* Small ubiquitin-like modifier modification regulates the DNA binding activity of glial cell missing *Drosophila* homolog a. *J. Biol. Chem.* **282**, 27239–27249 (2007).
40. Kerner, J. & Hoppel, C. Fatty acid import into mitochondria. *Biochim. Biophys. Acta* **1486**, 1–17 (2000).
41. Sebastian, D., Herrero, L., Serra, D., Asins, G. & Hegardt, F.G. CPT I overexpression protects L6E9 muscle cells from fatty acid–induced insulin resistance. *Am. J. Physiol. Endocrinol. Metab.* **292**, E677–E686 (2007).
42. Dobbins, R.L. *et al.* Prolonged inhibition of muscle carnitine palmitoyltransferase-1 promotes intramyocellular lipid accumulation and insulin resistance in rats. *Diabetes* **50**, 123–130 (2001).
43. Vidal-Puig, A.J. *et al.* Energy metabolism in uncoupling protein 3 gene knockout mice. *J. Biol. Chem.* **275**, 16258–16266 (2000).
44. Bezaire, V., Seifert, E.L. & Harper, M.E. Uncoupling protein-3: clues in an ongoing mitochondrial mystery. *FASEB J.* **21**, 312–324 (2007).
45. Brand, M.D. & Esteves, T.C. Physiological functions of the mitochondrial uncoupling proteins UCP2 and UCP3. *Cell Metab.* **2**, 85–93 (2005).
46. Rosenfeld, M.G., Lunyak, V.V. & Glass, C.K. Sensors and signals: a coactivator/corepressor/epigenetic code for integrating signal-dependent programs of transcriptional response. *Genes Dev.* **20**, 1405–1428 (2006).
47. Barish, G.D., Narkar, V.A. & Evans, R.M. PPARδ: a dagger in the heart of the metabolic syndrome. *J. Clin. Invest.* **116**, 590–597 (2006).
48. Lee, C.H. *et al.* PPARδ regulates glucose metabolism and insulin sensitivity. *Proc. Natl. Acad. Sci. USA* **103**, 3444–3449 (2006).




*Endocrine Journal* 2008, **55** (4), 767–776

NOTE

# Impact of Increased PPARγ Activity in Adipocytes *in vivo* on Adiposity, Insulin Sensitivity and the Effects of Rosiglitazone Treatment

KATSUKO TAKASAWA*, NAOTO KUBOTA*,**, YASUO TERAUCHI*** AND TAKASHI KADOWAKI*,**

**Department of Metabolic Diseases, Graduate School of Medicine, University of Tokyo, Tokyo 113-8655, Japan*
***Division of Applied Nutrition, National Institute of Health and Nutrition, Tokyo 162-8636, Japan*
****Department of Endocrinology and Metabolism, Graduate School of Medicine, Yokohama City University, Yokohama 236-0004, Japan*

**Abstract.** Peroxisome proliferator-activated receptor (PPAR)γ, a transcription factor belonging to the nuclear receptor superfamily, is essential for adipogenesis. PPARγ is recognized as a major target for the insulin-sensitizing effects of the thiazolidinediones. Previous studies have demonstrated that heterozygous PPARγ-deficient mice are protected from high-fat diet (HFD)-induced adipocyte hypertrophy, obesity and insulin resistance, which suggests that PPARγ may have a pivotal role in adipocyte hypertrophy, obesity and insulin resistance. In this study, we generated transgenic mice with the gain-of-function PPARγ Ser112Ala mutation (S112A mice) using the aP2 promoter, to elucidate the impact of increased PPARγ activity in mature adipocytes. Despite a 2–3-fold increase in the adipocyte PPARγ2 gene expression and PPARγ activity, the S112A mice showed comparable adiposity and insulin sensitivity to wild-type mice under both normal and HFD conditions. Although the expression levels of the PPARγ target genes involved in lipid metabolism, such as aP2 and stearoyl-CoA desaturase 1, were upregulated in the white adipose tissue of the S112A mice, the serum levels of free fatty acid, triglyceride, adiponectin and leptin, as well as the oxygen consumption, were comparable between the wild-type and S112A mice under the HFD condition. Moreover, treatment with rosiglitazone ameliorated insulin resistance and glucose intolerance to a similar degree in the two genotypes under the HFD condition. In conclusion, whereas the 50% decrease in PPARγ activity showed protection from HFD-induced obesity and insulin resistance, in the present study, the 2–3-fold increase in PPARγ2 expression and PPARγ activity failed to show obesity and insulin resistance even under the HFD condition.

*Key words*: Peroxisome proliferator-activated receptor γ, Rosiglitazone

(*Endocrine Journal* **55**: 767–776, 2008)

**PEROXISOME** proliferator-activated receptor (PPAR)γ, a member of the nuclear hormone receptor family of transcription factors, plays a central role in adipogenesis and lipid storage [1]. PPARγ exists as two isoforms, PPARγ1 and PPARγ2 [2]. While PPARγ1 is known to be expressed in several tissues, PPARγ2 expression is mainly restricted to the adipose tissue [1].

Previous studies have demonstrated that heterozygous PPARγ-deficient mice are protected from high-fat diet (HFD)-induced adipocyte hypertrophy, obesity and insulin resistance [3, 4], which suggests that PPARγ may have a pivotal role in adipocyte hypertrophy and insulin resistance. Consistent with this, a polymorphism of the human PPARγ2 gene, Pro12Ala, which decreases PPARγ activity, was shown to be associated with enhanced insulin sensitivity and a lower body mass index [5, 6]. In addition, partial PPARγ antagonists decreased the triglyceride (TG) content in white adipose tissue (WAT), skeletal muscle and liver, and ameliorated HFD-induced obesity and insulin resistance [7]. Thus, moderately reduced PPARγ activity was shown to be associated with improvement of insulin sensitivity.

The thiazolidinediones (TZDs), synthetic PPARγ

Received: January 17, 2008
Accepted: January 21, 2008
Correspondence to: Takashi KADOWAKI, M.D., Ph.D., Department of Metabolic Diseases, Graduate School of Medicine, University of Tokyo, 7-3-1 Hongo, Bunkyo-ku, Tokyo 113-8655, Japan

ligands, are widely used in the treatment of type 2 diabetes [1]. TZD-induced PPARγ activation increases the plasma levels of the insulin-sensitizing adipokine, adiponectin [8], and simultaneously decreases the plasma levels of free fatty acid (FFA) and insulin-resistance-causing adipokines such as TNFα and resistin [8]. Thus, PPARγ activation by TZD ameliorates insulin resistance, whereas heterozygous PPARγ-deficient mice are protected from HFD-induced adipocyte hypertrophy, obesity and insulin resistance [3, 4].

PPARγ activity is regulated by mitogen-activated protein (MAP) kinase phosphorylation of the serine 112 residue, which reduces its transcriptional activity [9]. The PPARγ Ser112Ala (S112A) mutation has been shown to be non-phosphorylable and indeed more active than wild-type PPARγ [9]. S112A knock-in mice showed improved insulin sensitivity without body weight gain [10]. A gain-of-function PPARγ mutation in humans had no impact on the insulin resistance, but induced obesity [11]. These phenotypes can probably be explained by the induction of PPARγ expression in the early stage of differentiation of preadipocytes [12]. In contrast, overexpression of wild-type PPARγ in mature 3T3L1 adipocytes increased both the cell size and intracellular TG content [13]. Although expression of PPARγ2 is maintained at a high level even in mature adipocytes [14], the physiological role of increased PPARγ activity in mature adipocytes *in vivo* remains unknown.

To understand the role of increased PPARγ activity in mature adipocytes *in vivo*, we produced transgenic mice with the PPARγ2 S112A mutation to activate PPARγ under the aP2 promoter. Moreover, we examined the effect of increased PPARγ activity in mature adipocytes on TZD-induced amelioration of insulin sensitivity.

## Materials and Methods

*Generation of transgenic PPARγ2-S112A mutant mice*

The mouse PPARγ2 cDNA (1.8 kb) with the S112A mutation, generated by PCR mutagenesis, was subcloned into the *Kpn*I-*Sac*I site of pBluescript SK(–) (Stratagene, La Jolla, CA, USA). PPARγ2-S112A cDNA was ligated into the unique *Eco*RI site between the rabbit β-globin intron and the polyadenylation signal. The resultant fragment was ligated into the *Sma*I site of a plasmid containing the aP2 promoter in pBluescript SK(–). The DNA fragment was excised from its plasmid by digestion with *Cla*I-*Not*I, then purified and microinjected into the pronuclei of fertilized eggs obtained from C57Bl/6N mice (Nippon CREA Co. Ltd., Tokyo, Japan). Transgenic founder mice were identified by Southern blot analysis of tail DNAs. F1 offspring were then crossed with C57Bl/6N mice to establish a transgenic lineage. Male mice with access to food *ad libitum* and reared under a light-dark cycle of 12 h were used for the experiments at 8–10 weeks of age. All experimental procedures conformed to the guidelines of the Animal Care Committee of the University of Tokyo.

*Genotyping by PCR*

Genotype was determined by PCR analysis of genomic DNA obtained from tail snips. To detect the S112A transgene, the sense primer corresponded to sequences in the rabbit β-globin intron (5'-TTATTG GTAGAAACAACTACATCCT-3'), and the antisense primer corresponded to sequences in the coding region of PPARγ (5'-ATATTTGTAATCAGCAACCATTG GG-3'). To detect the wild-type allele, the sense primer corresponding to sequences in the coding region of PPARγ (5'-AACTTCGGAATCAGCTCTGTGGACC-3') and the same antisense primer as that indicated above for detection of the S112A transgene, were used. The three primers and a genomic DNA template were mixed in a tube. The thermal reaction cycles consisted of an initial step at 94°C for 5 min, followed by 35 cycles of 94°C for 30 seconds, 55°C for 1 min and 72°C for 1 min, with a final step at 72°C for 5 min. The wild-type allele yielded a 393 base-pair (bp) product, and the transgene, a 529 bp product.

*In vivo glucose homeostasis*

Glucose tolerance test: The mice were fasted for more than 16 h before the study. They were then given 1.0 mg/gram (body weight) of glucose orally. Blood samples were collected at different time-points and the blood level of glucose was measured immediately with an automatic blood glucose meter (Glutest Pro: Sanwa Chemical, Nagoya, Japan). Whole blood specimens were collected and centrifuged, and the serum samples obtained after separation were stored at –20°C. Insulin levels were determined with an insulin

radioimmunoassay (RIA) kit (BIOTRAK: Amersham Biosciences, Buckinghamshire, UK) using rat insulin as the standard.

Insulin tolerance test: Mice were given free access to chow before the study. They were administered an intraperitoneal injection of 0.75 mU/gram (body weight) of human insulin (Humulin R: Lilly, Indianapolis, IN, USA). Blood samples were taken at different time-points from the tail vein and the blood levels of glucose were measured with an automatic blood glucose meter.

*RNA preparation, Northern blot analysis and real-time quantitative PCR*

Total RNA was prepared from epididymal WAT with TRIzol (invitrogen, Carlsbad, CA) according to the manufacturer's instructions. Northern blot analysis was performed using the standard protocol. A 20 μg sample of total RNA was electrophoresed through denaturing formaldehyde-agarose (1%) gel and then transferred to a Hybond $N^+$ nylon membrane (Amersham Biosciences). Real-time quantitative PCR was performed on an ABI Prism 7900 HT Sequence Detection System (Applied Biosystems, Foster City, CA) using TaqMan PCR Master Mix Reagent Kit (Applied Biosystems), with cyclophilin as the internal control. The primers and probe used for cyclophilin were as follows: forward, GGTCCTGGCATCTTGTC CAT; reverse, CAGTCTTGGCAGTGCAGATAAAA; probe, CTGGACCAAACACAAACGGTTCCCA. The primers and probes for the other genes were purchased from Applied Biosystems.

*Generation of probe and RNase protection assay (RPA)*

A partial murine PPARγ cDNA probe was generated by reverse transcriptase-PCR using total RNA and primers designed to amplify a region including 90 bp of the PPARγ2 transcript and a 185 bp region common to both PPARγ1 and PPARγ2, as previously described [15]. The PPARγ cDNA PCR product was subcloned into the *Pst*I-*Eco*RI site of the pBluescript SK(−) (Stratagene). The antisense cRNA was transcribed with [α-32P]UTP (PerkinElmer Life and Analytical Sciences, Inc., Boston, MA, USA) using the T7 RNA polymerase (MAXIscript: Ambion, Inc., Austin, TX, USA). A 10 μg sample of total RNA was subjected to RPA using an RPAIII kit (Ambion, Inc.) and hybridized overnight with the cRNA probe in Hybridization III Buffer (Ambion, Inc.) at 42°C. After digestion with RNaseA/RNaseT1 diluted 1 : 100, the protected fragments were separated on 8 M urea/5% polyacrylamide gels and analyzed quantitatively using an imaging plate and BAS2000 (Fuji Film, Tokyo, Japan).

*Diets and rosiglitazone treatment*

The normal diet (MF) was purchased from Oriental Yeast Co., Ltd. (Tokyo, Japan). The diet was composed of 5.3% (wt/wt) fat, 23.6% protein, 54.4% carbohydrate, 2.9% dietary fiber, and 6.1% minerals. The HFD, containing 32% safflower oil, 33.1% casein, 17.6% sucrose and 5.6% cellulose, was prepared as described previously [3]. Rosiglitazone (BRL49653), procured from GlaxoSmithKline (Brentford Middlesex, UK), was given at a 0.01% (wt/wt) mixture with the HFD.

*Histochemistry*

Epididymal adipose tissue was removed from each animal, fixed in 10% formaldehyde/PBS, and stored at 4°C until use. The tissue specimens were routinely processed for paraffin embedding, and 5-μm sections were cut and mounted on silanized slides. The adipose tissue was stained with hematoxylin and eosin, and the total adipocyte area was analyzed with Win ROOF software (Mitani Co., Ltd., Chiba, Japan). The white adipocyte area was measured in 400 or more cells per mouse in each group as described previously [3].

*Blood sample assays*

The serum levels of FFA and TG were determined by a nonesterified fatty acid-C test and triglyceride L-type test (Wako Pure Chemical Industries, Japan), respectively. The serum levels of adiponectin and leptin were assayed with a mouse adiponectin immunoassay kit (Otsuka Pharmaceutical, Tokushima, Japan) and Quantikine M kit (R&D Systems, Minneapolis, MN), respectively.

*Energy expenditure*

Oxygen consumption was measured every 3 minutes for 24 h in fasting mice using an $O_2/CO_2$ metabolism

measurement device (Model MK-5000; Muromachikikai, Tokyo, Japan). Each mouse was placed in a sealed chamber (560 ml volume) with an air flow rate of 500 ml/min at room temperature. The amount of oxygen consumed was converted to milliliters per minute by multiplying it with the flow rate.

*Statistical analysis*

Data were expressed as means ± SE. Differences between two groups were analyzed by Student's *t* test for unpaired comparisons. Individual comparisons among more than two groups were assessed with post-hoc Fisher's PLSD test. Differences were considered significant at $P<0.05$.

## Results

*Two-fold increase of PPARγ activity in the S112A mouse adipocytes*

Transgenic mice with the PPARγ2 S112A mutation expressed under the control of the aP2 promoter were established to investigate the physiological role of increased PPARγ activity in mature adipocytes (Fig. 1A). A 13.5 kb wild-type allele and a 1.2 kb mutant allele in the transgenic mice were identified by Southern blot analysis (Fig. 1B). Eleven founder mice carrying 2 to 10 copies of the transgene were produced and four lines of transgenes carrying 2 copies expressed PPARγ2 in the adipose tissue. While a 3-fold higher PPARγ2 mRNA expression was found in the S112A mouse than in the wild-type mouse adipose tissue, there was no significant difference in the expression level of PPARγ1 (Fig. 1C). The mRNA levels of aP2, stearoyl-CoA desaturase (SCD)1 and C/EBPα, downstream target genes of PPARγ, were significantly upregulated in the WAT of the S112A mice as compared with that in the wild-type mice (Fig. 1D), confirming that enhanced PPARγ activity in the S112A mice.

*S112A mice showed comparable WAT mass, insulin sensitivity and serum lipid levels to wild-type mice under the HFD condition*

S112A mice showed similar body weight, epididymal WAT mass and food intake to wild-type mice on a normal diet (data not shown). Administration of a HFD for 20 weeks, while inducing a 2-fold increase in the PPARγ2 expression in the WAT of the S112A mice (Fig. 2A), had no significant effect on the body weight, linear growth (Fig. 2B) or epididymal WAT mass (wild-type: 1.58 ± 0.14 g; S112A: 1.78 ± 0.17 g ($n = 7$)) of these mice. Histological analyses revealed that the adipocyte size in the WAT was not significantly different between the wild-type and S112A mice under either the normal or HFD condition (Fig. 2C). No differences in insulin sensitivity or glucose tolerance were found between the wild-type and S112A mice under either the normal (data not shown) or HFD condition (Fig. 2D and E). The serum FFA, TG, adiponectin and leptin levels were comparable between the wild-type and S112A mice mice under both normal and HFD conditions (Fig. 2F–I). Oxygen consumption was also similar between the two genotypes (Fig. 2J).

*Gene expressions in the WAT of the wild-type and S112A mice under the HFD condition*

We next investigated the expression of the genes involved in lipid metabolism in the WAT of the S112A mice. The expressions of aP2, lipoprotein lipase (LPL), acyl-CoA oxidase (ACO), SCD1 and hormone-sensitive lipase (HSL), whose promoters contain a peroxisome proliferator response element (PPRE), were upregulated in the S112A mice (Fig. 3A and B). The expression levels of CD36 remained unchanged, even though the CD36 promoter also contains a PPRE (Fig. 3A).

*Rosiglitazone increased the insulin sensitivity to a similar degree in both the mouse genotypes*

We examined the effects of rosiglitazone on the insulin sensitivity and glucose tolerance in the wild-type and S112A mice. The body weights of the wild-type and S112A mice were comparable, and rosiglitazone treatment did not change the body weight of either genotype (Fig. 4A). The adipocyte size was reduced to a similar degree in the wild-type and S112A mice after rosiglitazone treatment (Fig. 4B). Rosiglitazone significantly increased the insulin sensitivity to a similar degree in both the wild-type and S112A mice (Fig. 4C). Moreover, wild-type and S112A mice treated with rosiglitazone showed similar decreases of the blood glucose and insulin levels in the glucose toler-

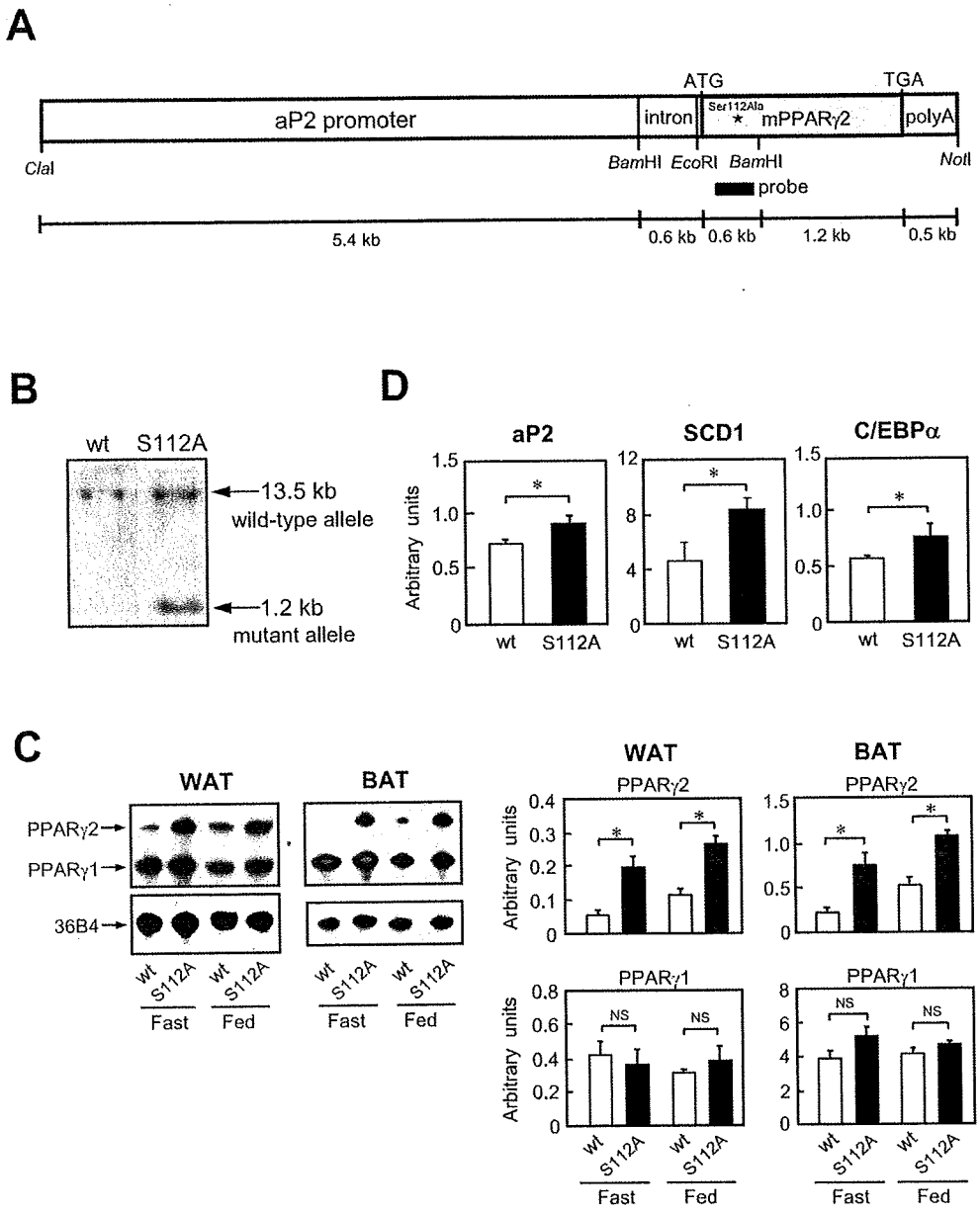


**Fig. 1.** Generation of transgenic mice expressing PPARγ2 with the S112A mutation. A, Schematic of the transgene and the probe used for Southern blot analysis. B, Southern blot analysis of *Bam*H1-digested mouse genomic DNA from wild-type (wt) and S112A mice hybridized with the probe, a 0.4 kb cDNA fragment. C, Expression of PPARγ mRNAs under the fed and 24 h fasting conditions as determined by RPA. PPARγ1 and PPARγ2 mRNAs are shown as protected bands of 185 and 273 bp, respectively. 36B4 RNA (220 bp protected band) was used as the internal control. D, TaqMan RT-PCR analyses of aP2, SCD1 and C/EBPα mRNAs after 24 h' fasting. Values are expressed as means ± S.E. ($n = 3$) *$P$<0.05. NS, no significant difference.

ance test (Fig. 4D). Rosiglitazone treatment significantly reduced the serum levels of FFA, but not TG, to a similar degree (Fig. 4E and F) in both the mouse genotypes. The serum adiponectin levels increased (Fig. 4G) and leptin levels decreased to a similar degree in both the mouse genotypes after rosiglitazone treatment (Fig. 4H). These data suggest that rosiglitazone increased the insulin sensitivity to a similar degree in the two genotypes.